Version of Record: https://www.sciencedirect.com/science/article/pii/S0375947421000245
Manuscript_eff2c7a2185a6f843a1ea2a0b252f9a5

Isoscalar and isovector giant resonances in ^{44}Ca, ^{54}Fe, ^{64,68}Zn and ^{56,58,60,68}Ni

G. Bonasera[1,*], S. Shlomo[1+], D.H. Youngblood[1], Y.-W. Lui[1], J. Button[1], and X. Chen[2]

[1]Cyclotron Institute, Texas A&M University, College Station, Texas 77843, USA

[2]Department of Radiation Oncology, Medical College of Wisconsin, Milwaukee, Wisconsin 53226, USA

(Dated: July 2020)

We have studied the uncharacteristic behavior of the measured values of the isoscalar and isovector centroid energies, E_{CEN}, of nuclear giant resonances of multipolarity from L=0 to L=3 in ^{44}Ca, ^{54}Fe, ^{64,68}Zn and ^{56,58,60,68}Ni. For this purpose, we carried out calculations of E_{CEN} within the spherical Hartree-Fock (HF)-based random phase approximation (RPA) theory with 33 distinct Skyrme-like effective nucleon-nucleon interactions. We have also determined the Pearson linear correlation coefficients between centroid energies, obtained from the HF-RPA, and the various properties of nuclear matter (NM) of each interaction and determined the sensitivity of E_{CEN} to NM properties. We compared the theoretical values of E_{CEN} obtained from the HF-RPA calculations with experimental data and discuss the results, pointing out significant disagreements between theoretical and experimental values. We note in particular, that we obtain good agreement for the theoretical E_{CEN} of the isovector giant dipole resonance and the available experimental data.

PACS number(s): 24.30.Cz, 21.60.Jz, 21.65.-f, 27.40.+z

* giacomo90@email.tamu.edu

+ s-shlomo@tamu.edu

I. INTRODUCTION

Nuclear giant resonances are an example of collective motion in the atomic nucleus and have been studied for many decades[1–5]**.** Nuclear giant resonances are classified in two modes of oscillation, neutrons and protons moving in-phase with each other (T=0, isoscalar) or out-of-phase (T=1, isovector) and of various multipolarities (L=0 monopole, L=1 dipole, and so on). The goal of these studies has been to determine, with ever increasing accuracy, the values of bulk nuclear matter (NM) properties in order to constrain the adopted form of the energy density functional (EDF) as well as the nucleon-nucleon interaction. The improved EDFs can then be used to determine better equations of state of nuclear matter, in order to estimate nuclear properties at and away from stability, properties of nuclear structure, dynamics of astrophysical and of heavy-ion reaction processes [6–10].

Similar to our previous studies, in which we analyzed the behavior of giant resonances across a wide range of masses from ^{40}Ca to ^{208}Pb[11] and then focused on the region A = 90-100 for isotopes of Mo and Zr[12–14], we now focus on the lower-mass region containing the ^{44}Ca, ^{54}Fe, ^{64,68}Zn and ^{56,58,60,68}Ni nuclei. We carried out calculations of centroid energies, E_{CEN}, using the Hartree-Fock (HF)-basis and random phase approximation (RPA) adopting 33 Skyrme-like effective interactions [15–17], for both the isoscalar and isovector (T=0 and T=1, respectively) giant resonances of multipolarities from L=0 to L=3. We also compare our results with available experimental data including that recently obtained at Texas A&M University for ^{44}Ca, ^{54}Fe, ^{64,68}Zn [18,19] as well as older data for the ^{58,60}Ni isotopes[20]**.** This investigation is an extension of our study [18,19] involving these nuclei in which we presented experimental data as well as

calculations employing only the KDE0v1[21] Skyrme-type interaction and compared both strength functions and centroid energies to the experimental data. In the following we describe our main results of significant disagreements obtained between theoretical and experimental values.

In the following section we briefly describe the theoretical background for determining the centroid energies, E_{CEN}, of T=0 and T=1 giant resonances from L=0 to L=3. Our results are compared with experimental data in section III where we present the calculated values of E_{CEN} for all nuclei for each giant resonance separately. Here we also study the sensitivity between the values of E_{CEN} and NM properties by determining the corresponding Pearson linear correlation coefficients. In Section IV we present and discuss our main results of the disagreement between the theoretical and experimental values of the centroid energies, E_{CEN}, of giant resonances and provide our concluding remarks.

II. METHOD

In our calculations we adopt the standard (10-parameter) Skyrme effective nucleon-nucleon interaction[22]*:*

$$V_{ij} = t_0\left(1 + x_0 P_{ij}^{\sigma}\right)\delta\left(\vec{r}_i - \vec{r}_j\right) + \frac{1}{2}t_1\left(1 + x_1 P_{ij}^{\sigma}\right)\left[\overleftarrow{k}_{ij}^{2}\delta\left(\vec{r}_i - \vec{r}_j\right) + \delta\left(\vec{r}_i - \vec{r}_j\right)\vec{k}_{ij}^{2}\right]$$
$$+ t_2\left(1 + x_2 P_{ij}^{\sigma}\right)\overleftarrow{k}_{ij}\delta\left(\vec{r}_i - \vec{r}_j\right)\vec{k}_{ij} + \frac{1}{6}t_3\left(1 + x_3 P_{ij}^{\sigma}\right)\rho^{\alpha}\left(\frac{\vec{r}_i + \vec{r}_j}{2}\right)\delta\left(\vec{r}_i - \vec{r}_j\right) \quad (1)$$
$$+ iW_0\overleftarrow{k}_{ij}\delta\left(\vec{r}_i - \vec{r}_j\right)\left(\vec{\sigma}_1 + \vec{\sigma}_2\right) \times \vec{k}_{ij} ,$$

where t_i, x_i, W_0 and α are the Skyrme parameters listed in TABLE I of reference[11]**.** The spin exchange operator is given by P_{ij}^{σ}, the Pauli spin operator is $\vec{\sigma}_i$ and lastly the left and right momentum operators are given by $\vec{k}_{ij} = -\frac{i(\vec{\nabla}_i - \vec{\nabla}_j)}{2}$ and $\overleftarrow{k}_{ij} = -\frac{i(\overleftarrow{\nabla}_i - \overleftarrow{\nabla}_j)}{2}$, respectively.

A more detailed description of the theoretical background can be found in Refs.[11,23–

25]. In this work we perform spherically symmetric Hartree-Fock (HF)-based random-phase approximation (RPA) calculations of strength functions S(E) and consequently determine the centroid energies. The strength function is defined by the sum over all RPA states $|n\rangle$ of energy E_n as

$$\mathrm{S(E)} = \sum_n |\langle 0|F_\mathrm{L}|n\rangle|^2 \delta(E_n - E_0). \quad (2)$$

In Eq. (2) the electromagnetic single-particle scattering operator, $\mathrm{F_L}$, takes the form $F_L = \sum_i f(r_i) Y_{L0}(i)$ or $\frac{Z}{A}\sum_n f(r_n) Y_{L0}(n) - \frac{N}{A}\sum_p f(r_p) Y_{L0}(p)$ for the T=0 or the T=1 excitations, respectively. The various multipolarities are determined by the operator $f(r)$: for the T = 0 and 1 monopole (L = 0) and quadrupole (L = 2) $f(r) = r^2$, for the octupole (L = 3) $f(r) = r^3$, for the isovector dipole (T = 1, L = 1) $f(r) = r$,while the isoscalar dipole (T = 0, L = 1) is obtained from $f(r) = r^3 - (5/3)\langle r^2\rangle r$ where we have subtracted the contribution from the spurious state [26,27]. The energy moments, m_k, of the strength function are integrated within the appropriate energy range Ω_1 to Ω_2:

$$m_k = \int_{\Omega_1}^{\Omega_2} E^k \mathrm{S(E)}\, dE \quad (3)$$

from which we determine the centroid energy:

$$\mathrm{E_{CEN}} = \frac{m_1}{m_0}. \quad (4)$$

In the RPA calculations we carry all the components of the interaction from the HF to ensure self-consistency [28]. Similar to previous publications, we approximate the single-particle orbits for the open-shell nuclei with a partial occupation numbers to account for the effect of pairing. It is well established that this is a good approximation for the strength functions for excitation energies in the giant resonance regions, resulting in centroid energies within less than 0.3 MeV of the energies obtained by including the effect of pairing, see for example, Ref.[29] and the online documentation of the TDHF code Sky3D[30]**.** The parameters of each Skyrme interaction used in this work are defined in Table I of reference[11] while the condition for the application of each are presented in Table II of reference[11]. An extended discussion can be found in Section II of Ref.[24]. We setup our calculations of the strength in a box with 100 grid points separated each by 0.2 fm. The maximum cutoff single particle energy was 100, 80, 50 and 50 MeV for multipolarities L = 0, 1, 2 and 3, respectively. The calculations of the energy moments were carried out using Γ= 0.1 MeV, for the Lorentzian distribution imposed onto the strength

function S(E), within the energy ranges shown in Table I. In Eq. (3) we have adopted the experimental excitation energy range when available and otherwise, a wide enough range to account for 100% of the energy weighted sum rule of the corresponding giant resonance, see Ref. [12] for detailed of the numerical calculations. The values of E_{CEN} that we obtained are numerically accurate to within 0.1 MeV.

III. RESULTS

We have calculated the isoscalar and isovector centroid energies, E_{CEN}, of multipolarity L=0-3, within the HF-based RPA approximation adopting 33 standard-form Skyrme-like effective interactions, for the nuclei ^{44}Ca, ^{54}Fe, ^{64,68}Zn, ^{56,58,60,68}Ni. The following interactions were employed in the calculations: SGII [31], KDE0[21], KDE0v1[21], SKM*[32], SK255[33], SkI3[34], SkI4[34], SkI5[34], SV-bas [35], SV-min [35], SV-sym32 [35], SV-m56-O [36], SV-m64-O [36], SLy4 [37], SLy5 [37], SLy6 [37], SkMP [38], SkO [39], SkO' [39], LNS [40], MSL0 [41], NRAPR [42], SQMC650 [43], SQMC700 [43], SkT1 [44], SkT2 [44], SkT3 [44], SkT8[44], SkT9 [44], SkT1* [44], SkT3* [44], Skxs20 [45] and Zσ [46].

These Skyrme interactions cover wide ranges of values of bulk nuclear matter properties. To study possible correlations among these properties, we have carried out calculation of Pearson linear correlation coefficients between these bulk values, which are presented in Table V of Ref. [11] and pointed out some weak possible correlations between bulk properties. We have also calculated the Pearson linear correlation coefficient, C, for the centroid energies, E_{CEN}, of every giant resonance and every one of the NM properties: the incompressibility coefficient $K_{NM} = 9\rho_0^2 \frac{\partial^2 E_0}{\partial \rho^2}|_{\rho_0}$, where $E_0[\rho]$ is the binding energy per nucleon and ρ_0 is the saturation density, the effective mass m*/m, the symmetry energy coefficients at ρ_0: $J = E_{sym}[\rho_0]$, and the

first and second derivatives $L = 3\rho_0 \left.\frac{\partial E_{sym}}{\partial \rho}\right|_{\rho_0}$ and $K_{sym} = 9{\rho_0}^2 \left.\frac{\partial^2 E_{sym}}{\partial \rho^2}\right|_{\rho_0}$, respectively, κ, the enhancement coefficient of the energy weighted sum rule (EWSR) of the isovector giant dipole resonance (IVGDR), and W_0, the strength of the spin-orbit interaction. We determined the sensitivity of E_{CEN} to bulk properties of NM. For two quantities, x and y, the Pearson linear correlation coefficient is determined by:

$$C = \frac{\sum_{i=1}^{n}(x_i - \bar{x})(y_i - \bar{y})}{\sqrt{\sum_{i=1}^{n}(x_i - \bar{x})^2}\sqrt{\sum_{i=1}^{n}(y_i - \bar{y})^2}} \quad (4)$$

where $\bar{x}$ and $\bar{y}$ are the averages of x and y and the sum runs over all interactions (n = 33). We adopt the same classification for the degree of correlation as in our previous work[11]: strong (|C| > 0. 80), medium (|C| = 0.61 – 0.80), weak (|C| = 0.35 – 0.60) and no correlation (|C| < 0.35).

In the sub-sections that follow we discuss the calculated results for giant resonances of multipolarity from L=0 to L=3, beginning with the isoscalar giant resonances and then the isovector giant resonances. We compare our results with the results of the experiments summarized in Table II. We note that isotopes of ^{56,68}Ni are unstable and the data for the isoscalar centroid energies was acquired using inverse kinematics [47–49], whereas for the other isotopes considered here the isoscalar data was acquired at Texas A&M University using inelastic scattering of 240 MeV α-particles [18–20]. Further details about the experimental setup can be found in[14,50–53]. The experimental data of the isovector giant dipole resonance was taken from the online tabulation maintained by the Centre for Photonuclear Experiments (Moscow State University) [54]. In Table III we show the calculated Pearson linear correlation coefficient obtained for the centroid energies and the various nuclear matter properties calculated for each multipolarity.

A. Isoscalar giant monopole resonance

The calculated centroid energy, E_{CEN}, of the isoscalar giant monopole resonance (ISGMR), is plotted against the nuclear matter incompressibility coefficient, K_{NM}, of the corresponding interaction used in the HF-based RPA, in FIG. 1. Each nucleus is shown in its own panel, with the calculated values of E_{CEN} shown as full circles and the corresponding experimental data is contained within the dashed lines. Medium correlation was obtained for the theoretical values of E_{CEN} and K_{NM} (C~0.73). For ^{44}Ca, ^{54}Fe, ^{56,58}Ni and ^{64}Zn we find good agreement between the calculated E_{CEN} and the measured value with the interactions with values of K_{NM} between 200-240 MeV yielding the best overall results. These interactions were found to reproduce the ISGMR E_{CEN} very well across a wide range of masses[11]. We note however, that for ^{68}Zn, (and for ^{60}Ni) we find that the calculated value of E_{CEN} of all (most) the interactions are above the experimental results. We point out that in the case of ^{68}Zn the experimental value of E_{CEN} is much lower than that of other nuclei in the region. Lastly, for the E_{CEN} of ^{68}Ni we find that the prediction of most of the interactions for E_{CEN} are below the experimental result, requiring a value of $K_{NM,}$ above 240 MeV. In FIG. 2 we show the obtained values of E_{CEN} plotted against the effective mass, m*/m, for which no correlation was found (C ~ -0.26). No correlation was also found for the theoretical values of E_{CEN} and the symmetry energy coefficient, *J*, (C~ -0.04), see FIG. 3. Similarly, no correlation is found for the E_{CEN} and the first derivative of the symmetry energy, *L* (C ~ 0.16) or the second derivative, K_{sym} (C ~ 0.24), shown in FIG. 4. No correlation is obtained for the remaining nuclear matter properties or for W_0, see Table III. We note that in our other works with different nuclei, in Refs. [11,12], we found stronger correlations between the values of E_{CEN} of the ISGMR and the value of K_{NM} and of m*/m.

In FIG. 5a we show the values E_{CEN} of the ISGMR of ^{44}Ca, ^{54}Fe and ^{64,68}Zn as functions of the nucleon mass, A. The experimental data are delimited with solid vertical lines while the theoretical values are plotted as points (with lines connecting results of the same interaction to guide the eye). As can be seen from these figures most of the interactions predict a slight increase in the value of E_{CEN} going from ^{44}Ca to ^{54}Fe and then a steady decrease. The experimental result on the other hand is pretty constant for the first three nuclei and then

decreases for ^{68}Zn. In FIG. 5b we show a similar plot of the E_{CEN} of the ISGMR, but for the Ni isotopes, as a function of A. In the case of the theoretical results we find a steady decrease in the value of E_{CEN} with a kink for the ^{58}Ni isotope. In the experimental data on the other hand we see that the value of E_{CEN} is similar for ^{56,58}Ni, decreases slightly for ^{60}Ni and then increases again for ^{68}Ni.

B. Isoscalar giant dipole resonance

We plot in FIG. 6 the centroid energy, E_{CEN}, of the isoscalar giant dipole resonance (ISGDR) against K_{NM}. Each isotope is considered individually, the calculated values are shown as full circles while the experimental data is contained within the dashed lines. We obtained only a weak correlation between the theoretical values of the E_{CEN} and K_{NM} (C ~ 0.39) for this compression mode. On the other hand, for the effective mass m*/m we obtained a strong correlation with the theoretical E_{CEN} values, see FIG. 7 (C ~0.83). Experimental data is not available for ^{54}Fe and ^{56,68}Ni. As shown in the plot, all calculated values of E_{CEN} are several MeV lower than the results of experiments for ^{44}Ca and ^{58,60}Ni. In contrast, the calculated values of E_{CEN}, for all the interactions, are 1-4 MeV above the experimental result for E_{CEN} in ^{64,68}Zn. The experimental values of E_{CEN} for the Zn isotopes are up to 10 MeV below the reported values of the other nuclei considered here. In FIG. 8, we show the centroid energy of the ISGDR plotted against the symmetry energy coefficient, *J*. No correlations are found for the values of *J* and E_{CEN} (C ~ -0.17). Similarly, in the case of the 1st and 2nd derivatives of the symmetry energy *J* (*L* and K_{sym}, respectively) we find no correlation, C ~ 0.01 and C ~ 0.23, with the calculated values of E_{CEN}, respectively. Details are given in Table III.

In FIG. 5c we show the values of E_{CEN} of the ISGDR of ^{44}Ca, ^{54}Fe and ^{64,68}Zn as functions of their mass, A. We see here that the theory predicts the value of E_{CEN} to gently fluctuate in this region. We also find that theory reproduces the increase in the value of E_{CEN} for the Zn isotopes. However, the calculated E_{CEN} is above the experimental value by a few MeV. In FIG. 5d the E_{CEN} of the Ni isotopes are plotted as a function of A. We see that the theoretical calculations of E_{CEN} are relatively constant across this range of isotopes, while the experimental value of E_{CEN} for ^{58}Ni is lower than that of ^{60}Ni. No data is available for the unstable isotopes ^{56,68}Ni.

C. Isoscalar giant quadrupole resonance

The centroid energies resulting from the HF-RPA calculations (shown as full-circles) of the isoscalar giant quadrupole resonance (ISGQR) are shown in FIG. 9 against the effective mass, m*/m. The area between the dashed lines represents the results of the experiments for each of the nuclei considered here. Similar to our previous results for a wide range of nuclear masses[11], we obtained a strong correlation for the calculated values of E_{CEN} of the ISGQR and m*/m (C~-0.93). We find that the interactions with a smaller effective mass reproduce the experimental values of E_{CEN} for ^{44}Ca and ^{54}Fe the best (m*/m = 0.65-0.8), whereas for all the other nuclei a higher effective mass (m*/m=0.8-0.9) is in better agreement with the data, with some interactions with effective masses as high as m*/m=1 reproducing the E_{CEN} of ^{56,60}Ni and ^{64}Zn. We note that a reasonable agreement between the theoretical and experimental values of E_{CEN} for the considered nuclei is obtained for an interaction with a value of m*/m=0.85. In FIG. 10 we show the E_{CEN} of the ISGQR plotted against the incompressibility coefficient of nuclear matter, K_{NM}. We found that some interactions across the entire range of K_{NM} reproduce the experimental E_{CEN}. Moreover, the correlation between the value of E_{CEN} and K_{NM} is weak (C~0.40), and it is mainly due to the correlation between the nuclear matter properties K_{NM} and m*/m (more details in TABLE V of Ref.[11]). As far as the symmetry energy coefficients, *J*, *L* and K_{sym}, no correlation is found for the calculated values of E_{CEN} and either *J* or *L* (C ~ -0.05 and 0.15, respectively), while a weak correlation is obtained for the values of E_{CEN} and K_{sym} (C~0.41). We also obtained weak correlations for the calculated values of E_{CEN} and the enhancement factor, κ, of the energy weighted sum rule (EWSR) of the IVGDR (C~0.52).

In FIG. 5e we show the values of E_{CEN} of the ISGQR for ^{44}Ca, ^{54}Fe and ^{64,68}Zn as functions of their mass, A. We find that the calculated and the experimental results agree on an increase in the value of E_{CEN} from ^{44}Ca to ^{54}Fe and then a decrease for ^{64,68}Zn. This peculiar behavior was already noticed in our work over a wide range of nuclei in the case of the lighter

nuclei considered[11] but not in the region of A=90-100[12,55]. The value of the E_{CEN} for the Ni isotopes on the other hand, shown in FIG. 5f, seems to steadily decrease in the theoretical calculations but to stay more or less constant in the experimental result. We also reiterate the point made above, which can be clearly seen from FIG. 5e and f, that the interactions with a higher value of effective mass (therefore with a lower value of E_{CEN}) reproduce the data of the Zn and Ni isotopes while the experimental values of E_{CEN} for ^{44}Ca and ^{54}Fe are reproduced by Skyrme parametrizations with a smaller m*/m.

D. Isoscalar giant octupole resonance

We demonstrate in FIG. 11 a strong correlation between calculated HF-RPA centroid energies (shown as full-circles) of the isoscalar giant octupole resonance (ISGOR) and the effective mass m*/m (C ~ 0.89). As can be seen in the figure the theoretical calculations are above the dashed lines representing the experimental data, available only for ^{58,60}Ni. A similar result was obtained over a wide range of nuclei[11]. In FIG. 12 we plot the theoretical values of E_{CEN} against the incompressibility coefficient. No correlation was obtained in this case (C ~ 0.33). Similarly, we find no correlation between E_{CEN} and the symmetry energy coefficients *J*, *L* and K_{sym}, with C ~ -0.1, C ~ -0.01 and 0.23, respectively. We obtained weak correlations for the theoretical values of the centroid energy and the enhancement factor, κ (C ~ -0.58).

In FIG. 5g we show the theoretical values of E_{CEN} of the ISGOR for ^{44}Ca, ^{54}Fe and ^{64,68}Zn as functions of their mass, A. We find a zig-zag-like trend in this case, a peculiarity not seen in the mass A=90-100 region[12]. For the Ni isotopes, shown in FIG. 5h, we find an overall decrease of the E_{CEN} from the HF-RPA calculation with increasing A. Moreover, the experimental values of E_{CEN} for ^{58}Ni and ^{60}Ni are significantly lower than the theoretical values, with the E_{CEN} of ^{58}Ni below that of ^{60}Ni.

E. Isovector giant monopole resonance

We point out that one expects that the centroid energy E_{CEN} of the isovector giant

monopole resonance (IVGMR), which is an isovector compression mode, will be sensitive to the incompressibility coefficient, K_{NM}, and to the symmetry energy, *J* and its derivatives, *L* and K_{sym}. In FIG. 13 we show the theoretical E_{CEN} (full-circles) of the IVGMR as functions of K_{NM}. There is no experimental data for E_{CEN} of the IVGMR for the nuclei studied here. A majority of the interactions estimate the value of E_{CEN} to be between 28-35 MeV except for ^{54}Fe and ^{56}Ni for which several interactions predict a value of E_{CEN} as high as 38.5 MeV. As shown in the figure, no correlation is found for E_{CEN} of this isovector compression mode and K_{NM} (C ~ 0.22)**.** In FIG. 14 the calculated E_{CEN} is shown plotted against the effective mass. We obtain a medium correlation for the calculated centroid energies of the IVGMR and m*/m, with C ~ -0.64 for the nuclei considered. Next, we plot the calculated E_{CEN} against the symmetry energy coefficient, J, in FIG. 15. No correlation is obtained for the theoretical values of E_{CEN} for the IVGMR and *J* (C ~ -0.24). In FIG. 16**,** the centroid energies are plotted as a function of the enhancement coefficient, κ, of the EWSR of the IVGDR. The calculated Pearson correlation coefficient for the theoretical values of E_{CEN} and κ is C ~ 0.80, demonstrating a strong correlation between the two quantitates in agreement with our previous work over a wide range of nuclei [11]**.** The remaining correlation coefficients for the theoretical values of E_{CEN} and the various NM properties can be seen in Table III.

In FIG. 17 a, we plot the theoretical value of the E_{CEN} of the IVGMR as a function of mass number A for ^{44}Ca, ^{54}Fe and ^{64,68}Zn. We find that most interactions predict an increase in the value of E_{CEN} when going from ^{44}Ca to ^{54}Fe and then lower values for ^{64,68}Zn. Similarly, we find that many interactions predict a larger value of E_{CEN} for ^{68}Zn compared to its lighter isotope, ^{64}Zn, however the two values are very close to each other. In FIG. 17 b we show a similar plot to (a) but for the Ni isotopes. We see a decreasing trend as the mass increases. A particularly steep decrease from the unstable isotope ^{56}Ni to ^{58}Ni is obtained for the Skyrme-type interactions with higher values of the enhancement coefficient, κ.

F. Isovector giant dipole resonance

In FIG. 18, the theoretical values of E_{CEN} of the isovector giant dipole resonance (IVGDR) are plotted (full circles) against the symmetry energy coefficient, *J*. A weak correlation

is obtained for the theoretical values of E_{CEN} and J (with C ~ -0.39). Similarly, in FIG. 19 we plotted the calculated E_{CEN} against the enhancement coefficient, κ. A strong correlation is obtained for the theoretical values of E_{CEN} and κ (C ~ 0.80). As demonstrated in FIG. 19 the values of E_{CEN} of most of the interactions fall below the experimental data for ^{44}Ca with only the E_{CEN} of the interactions with a higher value of κ (> 0.6) coming close to the experimental result, and similarly for ^{56,60}Ni and ^{64}Zn. We obtained the opposite result for ^{54}Fe and ^{68}Zn, where we find that the experimental data for E_{CEN} is also reproduced by interactions with a smaller enhancement coefficient κ as low as 0.1. In ^{58,68}Ni we obtain good agreement between theory and experiment for interactions with a value of κ = 0.25-0.7. Overall, we find that interactions with a value of the enhancement coefficient κ = 0.25-0.7 are the best at reproducing all the nuclei considered, in agreement with our study over a wide range of masses[11]. In FIG. 20 we show the E_{CEN} plotted against the effective mass, m*/m. A medium correlation was obtained for the theoretical values of the E_{CEN} and the effective mass associated with the relative Skyrme interaction used for the calculation, with C ~ -0.62. The correlation coefficients for the remaining NM properties are shown in Table III.

In FIG. 17 c, the values E_{CEN} of the IVGDR are plotted as functions of the mass number A of the isotopes of ^{44}Ca, ^{54}Fe and ^{64,68}Zn. We found for these nuclei that the theoretical values of the centroid energies decrease smoothly as A increases, with some minor fluctuations for some interactions. The experimental result on the other hand shows some fluctuation with the E_{CEN} of ^{64}Zn higher than the E_{CEN} of ^{54}Fe. The centroid energy of the Ni isotopes is plotted as a function of A in FIG. 17 d. We found the theory to predicts the centroid energy of the unstable isotope ^{56}Ni to be lower than that of ^{58}Ni, then a smooth decrease in the value of E_{CEN} as A increases to 60 and 68. Experimentally however, the centroid energy of ^{58}Ni is below that of ^{56}Ni but roughly the same as ^{60}Ni, while ^{68}Ni is lower.

G. Isovector giant quadrupole resonance

We consider now the isovector giant quadrupole resonance (IVGQR). In this case no measurements of E_{CEN} exist for the nuclei considered here. The theoretical values of the centroid energy, E_{CEN}, (full circles) are plotted against the symmetry energy coefficient, J, in FIG. 21. We

obtained most of the theoretical values of the centroid energies of the isotopes considered between 24-35 MeV. A weak correlation was obtained for the theoretical values of E_{CEN} and J with a correlation coefficient C ~ -0.38. No correlations are found for the calculated values of E_{CEN} and the 1st or 2nd derivative of *J, L* and K_{sym} with C ~ -0.34 and C ~ -0.17, respectively. In FIG. 22 we show the calculated centroid energy plotted against the enhancement coefficient, κ. In this case we obtained a strong correlation (C ~ 0.81) between the two values. The calculated centroid energies are plotted against the effective mass in FIG. 23 for which we obtained a medium correlation (C ~ -0.73). As shown in Table III, no correlation is found for the theoretical results of E_{CEN} and the incompressibility coefficient of nuclear matter K_{NM}.

In FIG. 17 e, the calculated E_{CEN} of the IVGQR is plotted as a function of the mass number A for the isotopes of ^{44}Ca, ^{54}Fe and ^{64,68}Zn. In this case we found that the theoretical centroid energies for all 4 isotopes are predicted to decrease slowly as A increases. Similarly, in FIG. 17f we plot the E_{CEN} for the Ni isotopes as a function of mass A and found that a majority of the interactions adopted predict the centroid energy to slowly decreases as A is increasing.

H. Isovector giant octupole resonance

No experiments have measured the centroid energy, E_{CEN}, of the isovector giant octupole resonance (IVGOR) for the nuclei consider here. We show the theoretical centroid energy (full circles) plotted against the symmetry energy coefficient J in FIG. 24. The theoretical centroid energy values, associated with most of the interactions considered, were obtained in the range of 34-43MeV. No correlation was found for the theoretical values of E_{CEN} and *J* (C ~ -0.29). Similarly, for the 1st and 2nd derivatives of *J* (*L* and K_{sym}, respectively) we obtained the values of C ~ -0.18 and C ~ 0.01, respectively. In FIG. 25 we show the theoretical centroid energies plotted against the enhancement coefficient, κ. As can be seen from the figure we obtained a medium correlation for the theoretical values of E_{CEN} and κ with a value of C ~ 0.79. In FIG. 26 we show the calculated values of E_{CEN} plotted against the effective mass. Strong correlations were determined for the theoretical E_{CEN} and the effective mass, with a value of C ~ -0.82. No correlation was found for the theoretical values of E_{CEN} and K_{NM} (C ~ 0.23).

The theoretical values of E_{CEN} for the IVGOR are shown as a function of nuclear mass number A for ^{44}Ca, ^{54}Fe and ^{64,68}Zn in FIG. 17g while the Ni isotopes are shown in FIG. 17h. In both cases we find a slow decrease in the value of E_{CEN} as A increases. However, for the Ni isotopes, we found that some interactions predict the E_{CEN} of ^{58}Ni to be above that of the unstable isotope ^{56}Ni.

IV. SUMMARY AND CONCLUDING REMARKS

In this work we presented results of fully self-consistent Hartree Fock based Random Phase Approximation calculations, within the spherical approximation, using the occupation number approximation for open shells. We employed 33 distinct Skyrme-like effective nucleon-nucleon interaction, and obtained the centroid energies, E_{CEN}, of both the isoscalar and isovector giant resonances of multipolarities from L=0 to L=3 for the isotopes of ^{44}Ca, ^{54}Fe, ^{64,68}Zn and ^{56,58,60,68}Ni. We compared our isoscalar results with the data recently obtained at Texas A&M University[18,19] and the ^{56,68}Ni experiments[20], while the isovector data was taken from the online 'Centre for photonuclear experimental data" maintained by Moscow State University[54]. It is important to point out when comparing the theoretical prediction of the 33 Skyrme interaction with experimental data that we have encountered important disagreements. In particular:

(i) For the isoscalar giant monopole resonance (ISGMR) we found for ^{44}Ca, ^{54}Fe, ^{56,58}Ni and ^{64}Zn good agreement between the calculated E_{CEN} and the measured values with the interactions associated with values of K_{NM} between 200-240 MeV. We note however, that for ^{68}Zn, (and for ^{60}Ni) the calculated values of E_{CEN} of all (most) the interactions are above the experimental results. The experimental value of E_{CEN} for ^{68}Zn is much lower than that of other nuclei in the region. Lastly, for ^{68}Ni the prediction of most of the interactions for E_{CEN} are below the experimental result, requiring a value of K_{NM} above 240 MeV.

(ii) For the isoscalar giant dipole resonance (ISGDR) and the isoscalar giant octupole resonance (ISGOR), there is significant disagreement between theory and experiment. Surprisingly, for ^{44}Ca, ^{58,60}Ni the calculated centroid energies are significantly lower

than the experimental result, opposite to what we found in other nuclei studied[11,12]. The experimental result for the ISGOR centroid energy for ^{58,60}Ni on the other hand are significantly lower than the calculated values.

(iii) For the isoscalar giant quadruple resonance (ISGQR), we found that interactions with a lower value of effective mass reproduce the experimental values of E_{CEN} for ^{44}Ca and ^{54}Fe the best (m*/m = 0.65-0.8), whereas for all the other nuclei a higher effective mass (m*/m=0.8-0.9) is in better agreement with the data with some interactions with effective masses as high as m*/m=1.0 reproducing the E_{CEN} of ^{56,58,60}Ni and ^{64}Zn. We note that a reasonable agreement between the theoretical and experimental values of E_{CEN} for the considered nuclei is obtained for an interaction with a value of m*/m = 0.85.

(iv) For the isovector giant dipole resonance (IVGDR), we found that the values of E_{CEN} of most of the interactions fall below the experimental data for ^{44}Ca with only the E_{CEN} of the interactions with a higher value of κ (> 0.6) coming close to the experimental result. We obtained the opposite result for ^{54}Fe and ^{68}Zn, where we found that the experimental data for E_{CEN} is also reproduced by interactions with a smaller enhancement coefficient κ, as low as low as 0.1. Overall, we found that interactions with a value of the enhancement coefficient κ = 0.25-0.7 are the best at reproducing all the nuclei considered, in agreement with our study over a wide range of masses[11].

We determined the Pearson linear correlation coefficient, C, in order to quantify the sensitivity of the E_{CEN} obtained from the HF-RPA calculations of the giant resonance to the nuclear matter properties of the adopted Skyrme-type effective interaction given in Eq. (1).

We obtained the following correlations between the theoretical values of the centroid energy and the incompressibility coefficient of nuclear matter: medium correlation for the ISGMR, weak correlation for the ISGDR and no correlation for the IVGMR. Meanwhile, for the effective mass we obtained the following correlations with the theoretical values of the centroid energies: strong correlation with the isoscalar giant dipole, quadrupole, octupole and isovector giant octuple resonances, while medium correlation was obtained for the isovector giant monopole, dipole and quadrupole resonances. We also found strong correlations between the theoretical result for E_{CEN} and the enhancement coefficient, κ, of the EWSR of the IVGDR, for the isovector giant

monopole, dipole, and quadrupole resonances, while medium correlations is found for the IVGOR. For the symmetry energy coefficients J, its 1st derivative, L, and 2nd derivative, K_{sym}, we found at most weak correlations with the calculated E_{CEN} values of certain multipolarities. We note that we found slightly lower values for C in the set of nuclei considered in this work compared to the mostly larger mass region of nuclei we studied recently[11,12]. We note that for some of the nuclei considered in this work several different configurations (set of occupation numbers) were feasible, an effect not seen for the other nuclei we recently studied [11,12].

The significant disagreement between the theoretical and the experimental values of E_{CEN} for the ISGDR (particularly ^{44}Ca, ^{58,60}Ni) and ISGOR (data available only for ^{58,60}Ni) as well as marginal agreement in other cases (such as the ISGMR in ^{68}Zn) suggests further investigations could be useful. The calculations of the response functions could be carried beyond the mean-field approximation by including nuclear structure effects[56–59], while parametrized ground state density and semi-classical transition densities that were used in the analyses of the experimental data within the folding-model distorted wave Born approximation could be replaced with calculated HF-based RPA ground state and transition densities[26,60].

ACKNOWLEDGEMENT

This research was in part funded by the US Department of Energy under Grant No. DE-FG03-

93ER40773.

---

[1] A. Bohr, B.M. Mottelson, Nuclear Structure II, Benjamin, New York, 1975.

[2] P. Ring, P. Schuck, The nuclear many-body problem, Springer-Verlag, 1980.

[3] M.N. Harakeh, A. van der (Adriaan) Woude, Giant resonances : fundamental high-frequency modes of nuclear excitation, Oxford University Press, 2001. https://global.oup.com/academic/product/giant-resonances-9780198517337?cc=us&lang=en& (accessed August 20, 2018).

[4] S. Shlomo, V.M. Kolomietz, G. Colò, Deducing the nuclear-matter incompressibility coefficient from data on isoscalar compression modes, Eur. Phys. J. A. 30 (2006) 23–30. doi:10.1140/epja/i2006-10100-3.

[5] S. Shlomo, D.H. Youngblood, Nuclear matter compressibility from isoscalar giant monopole resonance, Phys. Rev. C. 47 (1993) 529–536. doi:10.1103/PhysRevC.47.529.

[6] N.K. Glendenning, Equation of state from nuclear and astrophysical evidence, Phys. Rev. C. 37 (1988) 2733–2743. doi:10.1103/PhysRevC.37.2733.

[7] J.M. Lattimer, M. Prakash, Neutron star observations: Prognosis for equation of state constraints, Phys. Rep. 442 (2007) 109–165. doi:http://dx.doi.org/10.1016/j.physrep.2007.02.003.

[8] S. Shlomo, V.M. Kolomietz, Hot nuclei, Reports Prog. Phys. 68 (2005) 1. doi:10.1088/0034-4885/68/1/R01.

[9] V.M. Kolomietz, S. Shlomo, Mean Field Theory, WORLD SCIENTIFIC, 2020.

doi:10.1142/11593.

[10] V.M. Kolomietz, A.I. Sanzhur, S. Shlomo, S.A. Firin, Equation of state and phase transitions in asymmetric nuclear matter, Phys. Rev. C. 64 (2001) 243151–243155. doi:10.1103/PhysRevC.64.024315.

[11] G. Bonasera, M.R. Anders, S. Shlomo, Giant Resonances in 40,48Ca, 68Ni, 90Zr, 116Sn, 144Sm and 208Pb, Phys. Rev. C. 98 (2018) 054316. doi:10.1103/PhysRevC.98.054316.

[12] G. Bonasera, S. Shlomo, D.H. Youngblood, Y.-W.W. Lui, Krishichayan, J. Button, Isoscalar and isovector giant resonances in 92,94,96,98,100Mo and 90,92,94Zr, Nucl. Phys. A. 992 (2019) 121612. doi:10.1016/j.nuclphysa.2019.121612.

[13] J. Button, Y.-W. Lui, D.H. Youngblood, X. Chen, G. Bonasera, S. Shlomo, Isoscalar E0 , E1 , E2 , and E3 strength in 94 Mo, Phys. Rev. C. 94 (2016) 034315. doi:10.1103/PhysRevC.94.034315.

[14] Krishichayan, Y.-W.W. Lui, J. Button, D.H.H. Youngblood, G. Bonasera, S. Shlomo, Isoscalar giant resonances in Zr 90,92,94, Phys. Rev. C. 92 (2015) 044323. doi:10.1103/PhysRevC.92.044323.

[15] T.H.R. Skyrme, CVII. The nuclear surface, Philos. Mag. 1 (1956) 1043–1054. doi:10.1080/14786435608238186.

[16] T.H.R. Skyrme, The effective nuclear potential, Nucl. Phys. 9 (1958) 615–634. doi:10.1016/0029-5582(58)90345-6.

[17] D. Vautherin, D.M. Brink, Hartree-Fock Calculations with Skyrme's Interaction. I. Spherical Nuclei, Phys. Rev. C. 5 (1972) 626–647. doi:10.1103/PhysRevC.5.626.

[18] J. Button, Y.-W. Lui, D.H. Youngblood, X. Chen, G. Bonasera, S. Shlomo, Isoscalar E0, E1, and E2 strength in ^{44}Ca, Phys. Rev. C. 96 (2017) 054330. doi:10.1103/PhysRevC.96.054330.

[19] J. Button, Y.W. Lui, D.H. Youngblood, X. Chen, G. Bonasera, S. Shlomo, Isoscalar E0, E1, and E2 strength in Fe 54 and Zn 64,68 Isoscalar E0, E1, and E2 Strength in ⋯ J. BUTTON et al., Phys. Rev. C. 100 (2019) 064318. doi:10.1103/PhysRevC.100.064318.

[20] Y.-W. Lui, D.H. Youngblood, H.L. Clark, Y. Tokimoto, B. John, Isoscalar giant resonances for nuclei with mass between 56 and 60, Phys. Rev. C. 73 (2006) 014314. doi:10.1103/PhysRevC.73.014314.

[21] B.K. Agrawal, S. Shlomo, V.K. Au, Determination of the parameters of a Skyrme type

effective interaction using the simulated annealing approach, Phys. Rev. C. 72 (2005) 014310. doi:10.1103/PhysRevC.72.014310.

[22] E. Chabanat, P. Bonche, P. Haensel, J. Meyer, R. Schaeffer, A Skyrme parametrization from subnuclear to neutron star densities, Nucl. Phys. A. 627 (1997) 710–746. doi:10.1016/S0375-9474(97)00596-4.

[23] T. Sil, S. Shlomo, B.K. Agrawal, P.-G. Reinhard, Effects of self-consistency violation in Hartree-Fock RPA calculations for nuclear giant resonances revisited, Phys. Rev. C. 73 (2006) 034316. doi:10.1103/PhysRevC.73.034316.

[24] M.R. Anders, S. Shlomo, T. Sil, D.H. Youngblood, Y.-W. Lui, Krishichayan, Giant resonances in 40Ca and 48Ca, Phys. Rev. C. 87 (2013) 024303. doi:10.1103/PhysRevC.87.024303.

[25] P.-G. Reinhard, From sum rules to RPA: 1. Nuclei, Ann. Phys. 504 (1992) 632–661. doi:10.1002/andp.19925040805.

[26] S. Shlomo, A.I. Sanzhur, Isoscalar giant dipole resonance and nuclear matter incompressibility coefficient, Phys. Rev. C. 65 (2002) 044310. doi:10.1103/PhysRevC.65.044310.

[27] B.K. Agrawal, S. Shlomo, A.I. Sanzhur, Self-consistent Hartree-Fock based random phase approximation and the spurious state mixing, Phys. Rev. C. 67 (2003) 034314. doi:10.1103/PhysRevC.67.034314.

[28] B.K. Agrawal, S. Shlomo, Consequences of self-consistency violations in Hartree-Fock random-phase approximation calculations of the nuclear breathing mode energy, Phys. Rev. C. 70 (2004) 014308. doi:10.1103/PhysRevC.70.014308.

[29] I. Hamamoto, H. Sagawa, X.Z. Zhang, Single-particle and collective properties of drip-line nuclei, Phys. Rev. C. 53 (1996) 765–774. doi:10.1103/PhysRevC.53.765.

[30] J.A. Maruhn, P.-G. Reinhard, P.D. Stevenson, A.S. Umar, The TDHF code Sky3D, Comput. Phys. Commun. 185 (2014) 2195–2216. doi:10.1016/J.CPC.2014.04.008.

[31] N. Van Giai, H. Sagawa, Spin-isospin and pairing properties of modified Skyrme interactions, Phys. Lett. B. 106 (1981) 379–382. doi:http://dx.doi.org/10.1016/0370-2693(81)90646-8.

[32] J. Bartel, P. Quentin, M. Brack, C. Guet, H.-B. Håkansson, Towards a better parametrisation of Skyrme-like effective forces: A critical study of the SkM force, Nucl.

Phys. A. 386 (1982) 79–100. doi:http://dx.doi.org/10.1016/0375-9474(82)90403-1.

[33] B.K. Agrawal, S. Shlomo, V. Kim Au, Nuclear matter incompressibility coefficient in relativistic and nonrelativistic microscopic models, Phys. Rev. C. 68 (2003) 031304. doi:10.1103/PhysRevC.68.031304.

[34] P.-G. Reinhard, H. Flocard, Nuclear effective forces and isotope shifts, Nucl. Phys. A. 584 (1995) 467–488. doi:http://dx.doi.org/10.1016/0375-9474(94)00770-N.

[35] P. Klupfel, P.-G. Reinhard, T.J. Burvenich, J.A. Maruhn, Variations on a theme by Skyrme: A systematic study of adjustments of model parameters, Phys. Rev. C. 79 (2009) 034310. doi:10.1103/PhysRevC.79.034310.

[36] N. Lyutorovich, V.I. Tselyaev, J. Speth, S. Krewald, F. Grümmer, P.-G. Reinhard, Self-Consistent Calculations of the Electric Giant Dipole Resonances in Light and Heavy Nuclei, Phys. Rev. Lett. 109 (2012) 092502. doi:10.1103/PhysRevLett.109.092502.

[37] E. Chabanat, P. Bonche, P. Haensel, J. Meyer, R. Schaeffer, A Skyrme parametrization from subnuclear to neutron star densities Part II. Nuclei far from stabilities, Nucl. Phys. A. 635 (1998) 231–256. doi:http://dx.doi.org/10.1016/S0375-9474(98)00180-8.

[38] L. Bennour, P.-H. Heenen, P. Bonche, J. Dobaczewski, H. Flocard, Charge distributions of 208Pb, 206Pb, and 205Tl and the mean-field approximation, Phys. Rev. C. 40 (1989) 2834–2839. doi:10.1103/PhysRevC.40.2834.

[39] P.-G. Reinhard, D.J. Dean, W. Nazarewicz, J. Dobaczewski, J.A. Maruhn, M.R. Strayer, Shape coexistence and the effective nucleon-nucleon interaction, Phys. Rev. C. 60 (1999) 014316. doi:10.1103/PhysRevC.60.014316.

[40] L.G. Cao, U. Lombardo, C.W. Shen, N. Van Giai, From Brueckner approach to Skyrme-type energy density functional, Phys. Rev. C. 73 (2006) 014313. doi:10.1103/PhysRevC.73.014313.

[41] L.-W. Chen, C.M. Ko, B.-A. Li, J. Xu, Density slope of the nuclear symmetry energy from the neutron skin thickness of heavy nuclei, Phys. Rev. C. 82 (2010) 024321. doi:10.1103/PhysRevC.82.024321.

[42] A.W. Steiner, M. Prakash, J.M. Lattimer, P.J. Ellis, Isospin asymmetry in nuclei and neutron stars, Phys. Rep. 411 (2005) 325–375. doi:http://dx.doi.org/10.1016/j.physrep.2005.02.004.

[43] P.A.M. Guichon, H.H. Matevosyan, N. Sandulescu, A.W. Thomas, Physical origin of

density dependent forces of Skyrme type within the quark meson coupling model, Nucl. Phys. A. 772 (2006) 1–19. doi:http://dx.doi.org/10.1016/j.nuclphysa.2006.04.002.

[44] F. Tondeur, M. Brack, M. Farine, J.M. Pearson, Static nuclear properties and the parametrisation of Skyrme forces, Nucl. Phys. A. 420 (1984) 297–319. doi:http://dx.doi.org/10.1016/0375-9474(84)90444-5.

[45] B.A. Brown, G. Shen, G.C. Hillhouse, J. Meng, A. Trzci, Neutron skin deduced from antiprotonic atom data, Phys. Rev. C. 76 (2007) 034305. doi:10.1103/PhysRevC.76.034305.

[46] J. Friedrich, P.-G. Reinhard, Skyrme-force parametrization: Least-squares fit to nuclear ground-state properties, Phys. Rev. C. 33 (1986) 335–351. doi:10.1103/PhysRevC.33.335.

[47] C. Monrozeau, E. Khan, Y. Blumenfeld, C.E. Demonchy, W. Mittig, P. Roussel-Chomaz, D. Beaumel, M. Caamaño, D. Cortina-Gil, J.P. Ebran, N. Frascaria, U. Garg, M. Gelin, A. Gillibert, D. Gupta, N. Keeley, F. Maréchal, A. Obertelli, J.-A. Scarpaci, M. Gelin, J.P. Ebran, W. Mittig, Y. Blumenfeld, J.-A. Scarpaci, F. Maréchal, C. Monrozeau, E. Khan, D. Beaumel, A. Obertelli, D. Cortina-Gil, P. Roussel-Chomaz, D. Gupta, N. Keeley, N. Frascaria, C.E. Demonchy, M. Caamaño, U. Garg, First Measurement of the Giant Monopole and Quadrupole Resonances in a Short-Lived Nucleus: Ni56, Phys. Rev. Lett. 100 (2008) 042501. doi:10.1103/physrevlett.100.042501.

[48] M. Vandebrouck, J. Gibelin, E. Khan, N.L. Achouri, H. Baba, D. Beaumel, Y. Blumenfeld, M. Caamaño, L. Càceres, G. Colò, F. Delaunay, B. Fernandez-Dominguez, U. Garg, G.F. Grinyer, M.N. Harakeh, N. Kalantar-Nayestanaki, N. Keeley, W. Mittig, J. Pancin, R. Raabe, T. Roger, P. Roussel-Chomaz, H. Savajols, O. Sorlin, C. Stodel, D. Suzuki, J.C. Thomas, Measurement of the Isoscalar Monopole Response in the Neutron-Rich Nucleus 68Ni, Phys. Rev. Lett. 113 (2014) 032504. doi:10.1103/PhysRevLett.113.032504.

[49] M. Vandebrouck, J. Gibelin, E. Khan, N.L. Achouri, H. Baba, D. Beaumel, Y. Blumenfeld, M. Caamaño, L. Càceres, G. Colò, F. Delaunay, B. Fernandez-Dominguez, U. Garg, G.F. Grinyer, M.N. Harakeh, N. Kalantar-Nayestanaki, N. Keeley, W. Mittig, J. Pancin, R. Raabe, T. Roger, P. Roussel-Chomaz, H. Savajols, O. Sorlin, C. Stodel, D. Suzuki, J.C. Thomas, Isoscalar response of <math> <mmultiscripts> <mi mathvariant="normal">Ni</mi> <mprescripts/> <none/> <mn>68</mn>

</mmultiscripts> </math> to <math> <mi>α</mi> </math> -particle and deuteron probes, Phys. Rev. C. 92 (2015) 024316. doi:10.1103/PhysRevC.92.024316.

[50] D.H. Youngblood, Y.-W. Lui, H.L. Clark, Isoscalar giant resonances in 28 Si and the mass dependence of nuclear compressibility, Phys. Rev. C. 65 (2002) 034302. doi:10.1103/PhysRevC.65.034302.

[51] Y.-W. Lui, H.L. Clark, D.H. Youngblood, Giant monopole strength in 58 Ni, Phys. Rev. C. 61 (2000) 067307. doi:10.1103/PhysRevC.61.067307.

[52] D.H. Youngblood, Y.-W. Lui, H.L. Clark, Giant resonances in 24 Mg, Phys. Rev. C. 60 (1999) 014304. doi:10.1103/PhysRevC.60.014304.

[53] D.H. Youngblood, Y.-W. Lui, Krishichayan, J. Button, G. Bonasera, S. Shlomo, Isoscalar E0, E1, E2, and E3 strength in 92,96,98,100Mo, Phys. Rev. C. 92 (2015) 014318. doi:10.1103/PhysRevC.92.014318.

[54] CDFE - CENTRE FOR PHOTONUCLEAR EXPERIMENTS DATA - HOME PAGE, CDFE - Cent. Photonuclear Exp. Data - HOME PAGE. (2019). http://cdfe.sinp.msu.ru (accessed February 20, 2019).

[55] D.H. Youngblood, Y.-W. Lui, Krishichayan, J. Button, M.R. Anders, M.L. Gorelik, M.H. Urin, S. Shlomo, Unexpected characteristics of the isoscalar monopole resonance in the $A \approx 90$ region: Implications for nuclear incompressibility, Phys. Rev. C. 88 (2013) 021301. doi:10.1103/PhysRevC.88.021301.

[56] S. Kamerdzhiev, J. Speth, G. Tertychny, Extended theory of finite Fermi systems: collective vibrations in closed shell nuclei, Phys. Rep. 393 (2004) 1–86. doi:10.1016/J.PHYSREP.2003.11.001.

[57] V.M. Kolomietz, S. Shlomo, Isoscalar compression modes within fluid dynamic approach, Phys. Rev. C. 61 (2000) 064302. doi:10.1103/PhysRevC.61.064302.

[58] D.C. Fuls, V.M. Kolomietz, S. V. Lukyanov, S. Shlomo, Damping effects on centroid energies of isoscalar compression modes, EPL (Europhysics Lett. 90 (2010) 20006. doi:10.1209/0295-5075/90/20006.

[59] V.M. Kolomietz, S. Shlomo, Nuclear Fermi-liquid drop model, Phys. Rep. 390 (2004) 133–233. doi:10.1016/j.physrep.2003.10.013.

[60] A. Kolomiets, O. Pochivalov, S. Shlomo, Microscopic description of excitation of nuclear isoscalar giant resonances by inelastic scattering of 240 MeV [Formula Presented]

particles, Phys. Rev. C. 61 (2000) 8. doi:10.1103/PhysRevC.61.034312.

Table I. Excitation energy ranges (in MeV) employed in the integration of the strength function distribution to obtain the desired centroid energies.

	^{44}Ca	^{54}Fe	^{56}Ni	^{58}Ni	^{60}Ni	^{64}Zn	^{68}Zn	^{68}Ni
L0T0	9 - 40	9 - 40	12 - 35	9 - 40	9 - 40	9 - 40	9 - 40	12 - 30
L1T0	20 - 40	20 - 40	20 - 40	20 - 40	20 - 40	20 - 40	20 - 40	20 - 40
L2T0	9 - 40	9 - 40	12 - 35	9 - 40	9 - 40	9 - 40	9 - 40	12 - 30
L3T0	15 - 40	15 - 40	15 - 40	15 - 40	15 - 40	15 - 40	15 - 40	15 - 40
L0T1	7 - 60	7 - 60	7 - 60	7 - 60	7 - 60	7 - 60	7 - 60	7 - 60
L1T1	0 - 60	0 - 60	0 - 60	0 - 60	0 - 60	0 - 60	0 - 60	0 - 60
L2T1	7 - 60	7 - 60	7 - 60	7 - 60	7 - 60	7 - 60	7 - 60	7 - 60
L3T1	25 - 60	25 - 60	25 - 60	25 - 60	25 - 60	25 - 60	25 - 60	25 - 60

Table II. Experimental values for the centroid energies (in MeV) of T=0 and 1 giant resonances. The isoscalar experimental data was found in the literature: Ref.[18] for a, Ref.[19] for b, Ref.[47] for c, Ref.[20] for d, Ref.[48] for e, and Ref.[49] for f. The isovector data was taken from the online 'Centre for photonuclear experimental data" maintained by Moscow State University[54].

	^{44}Ca	^{54}Fe	^{56}Ni	^{58}Ni	^{60}Ni	^{64}Zn	^{68}Zn	^{68}Ni
L0T0	19.49 (34) a	19.66 (37) b	19.30 (50) c	19.32 (32) d	18.10 (29) d	18.88 (79) b	16.60 (17) b	21.1 (19) e
L1T0	35.03 (145) a	-	-	34.06 (30) d	36.12 (28) d	25.66 (121) b	27.65 (39) b	-
L2T0	17.21 (48) a	18.05 (87) b	16.20 (50) c	16.34 (13) d	15.88 (14) d	15.85 (31) b	15.54 (32) b	15.9 (13) f

L3T0	-	-	-	23.20 (30) d	24.40 (26) d	-	-	-
L1T1	21.63 (50)	18.94 (50)	20.91 (50)	20.41 (50)	20.41 (50)	19.53 (50)	17.18 (50)	17.10 (20)

Table III. Pearson linear correlation coefficients, C, obtained for the centroid energies, resulting from the theoretical calculation for each giant resonance, and all of the nuclear matter properties at saturation density.

	K_{NM}	m*/m	$W_0(X_W=1)$	J	L	K_{sym}	κ
ISGMR	0.73	-0.26	-0.07	-0.04	0.16	0.24	0.02
ISGDR	0.39	-0.83	-0.02	-0.17	0.01	0.23	0.58
ISGQR	0.40	-0.93	0.07	-0.05	0.15	0.41	0.53
ISGOR	0.32	-0.89	0.04	-0.15	-0.01	0.24	0.58
IVGMR	0.22	-0.64	-0.12	-0.24	-0.13	-0.03	0.80
IVGDR	0.09	-0.62	-0.12	-0.39	-0.40	-0.27	0.80
IVGQR	0.17	-0.73	-0.13	-0.38	-0.34	-0.17	0.81
IVGOR	0.23	-0.82	-0.04	-0.29	-0.18	0.01	0.79

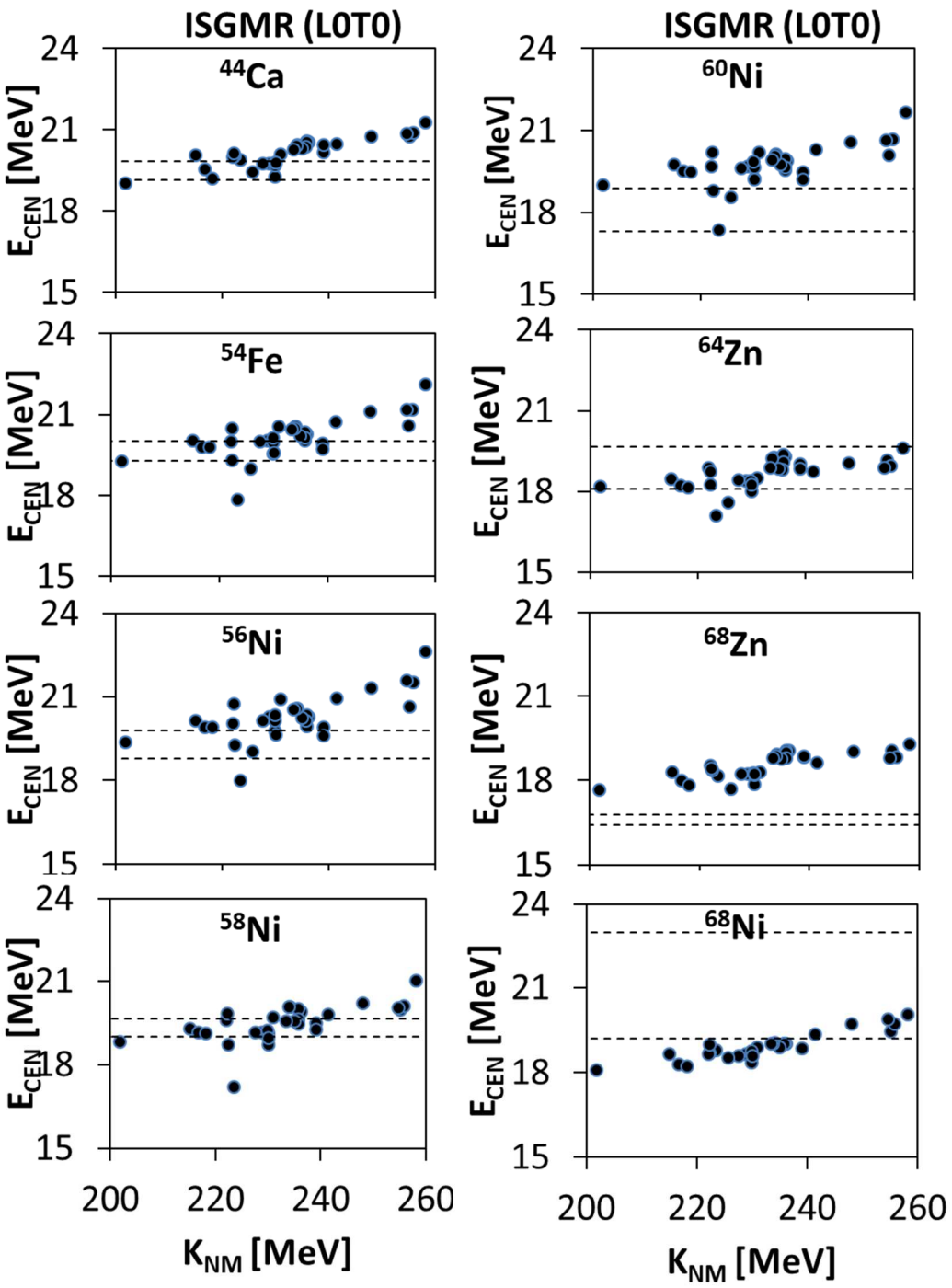

FIG. 1. Theoretical centroid energies, E_{CEN}, in MeV (full-circles) obtained from the HF-RPA calculations, of the isoscalar giant monopole resonance (ISGMR), for different Skyrme interactions, as a function of the incompressibility coefficient K_{NM}. Each nucleus has its own panel, the experimental uncertainties are contained by the dashed lines. We find a medium correlation between the values of E_{CEN} and K_{NM} with a Pearson linear correlation coefficient C ~ 0.73.

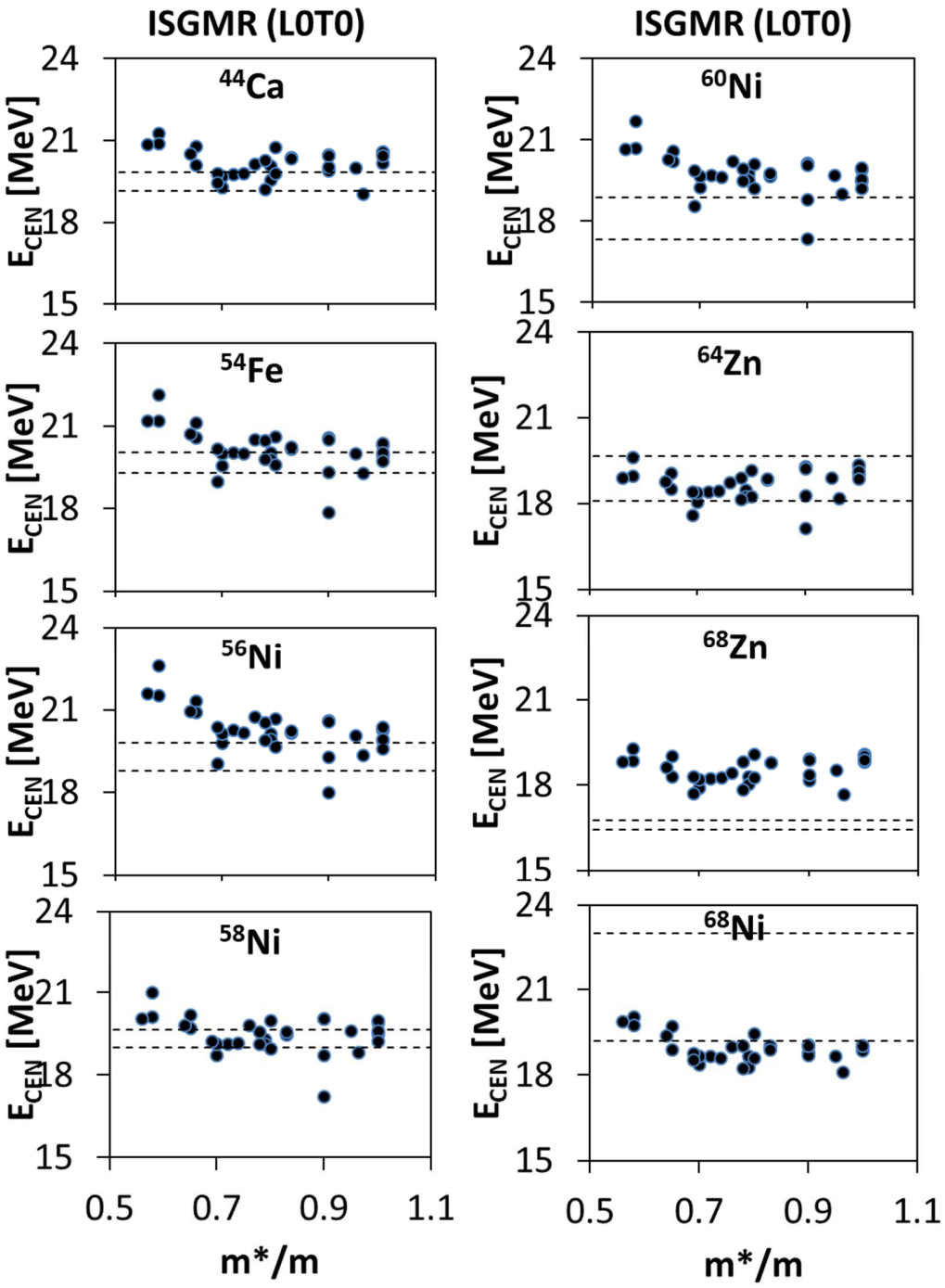

FIG. 2. As in FIG. 1 but we plot the centroid energy as a function of the effective mass. No correlation was found for the theoretical values of E_{CEN} and m*/m, with C ~ -0.26.

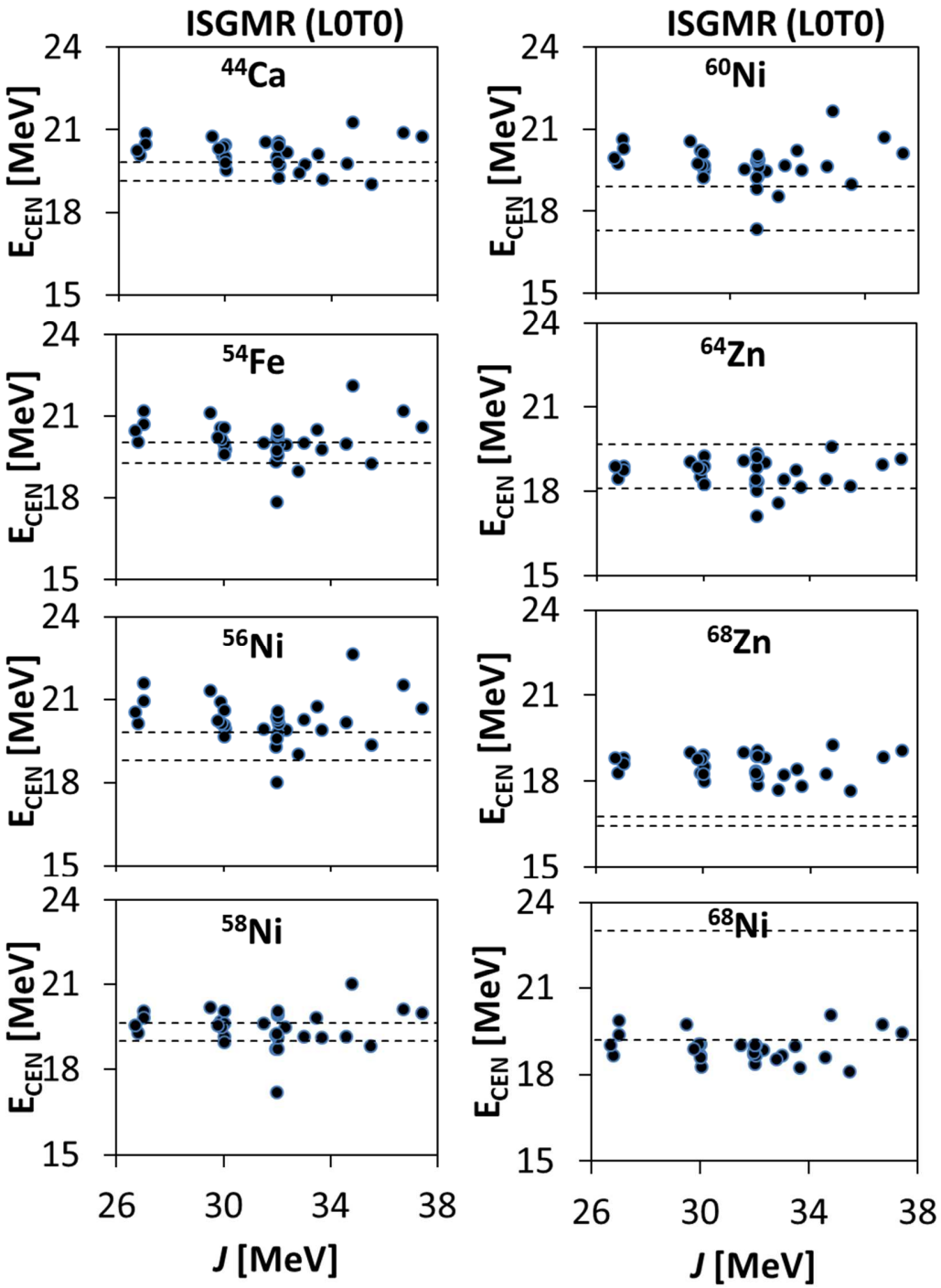

FIG. 3. As in FIG. 1 but we plot the centroid energy as a function of the symmetry energy, J, at saturation energy. No correlations are found for the theoretical values of E_{CEN} and J, with C ~ -0.04.

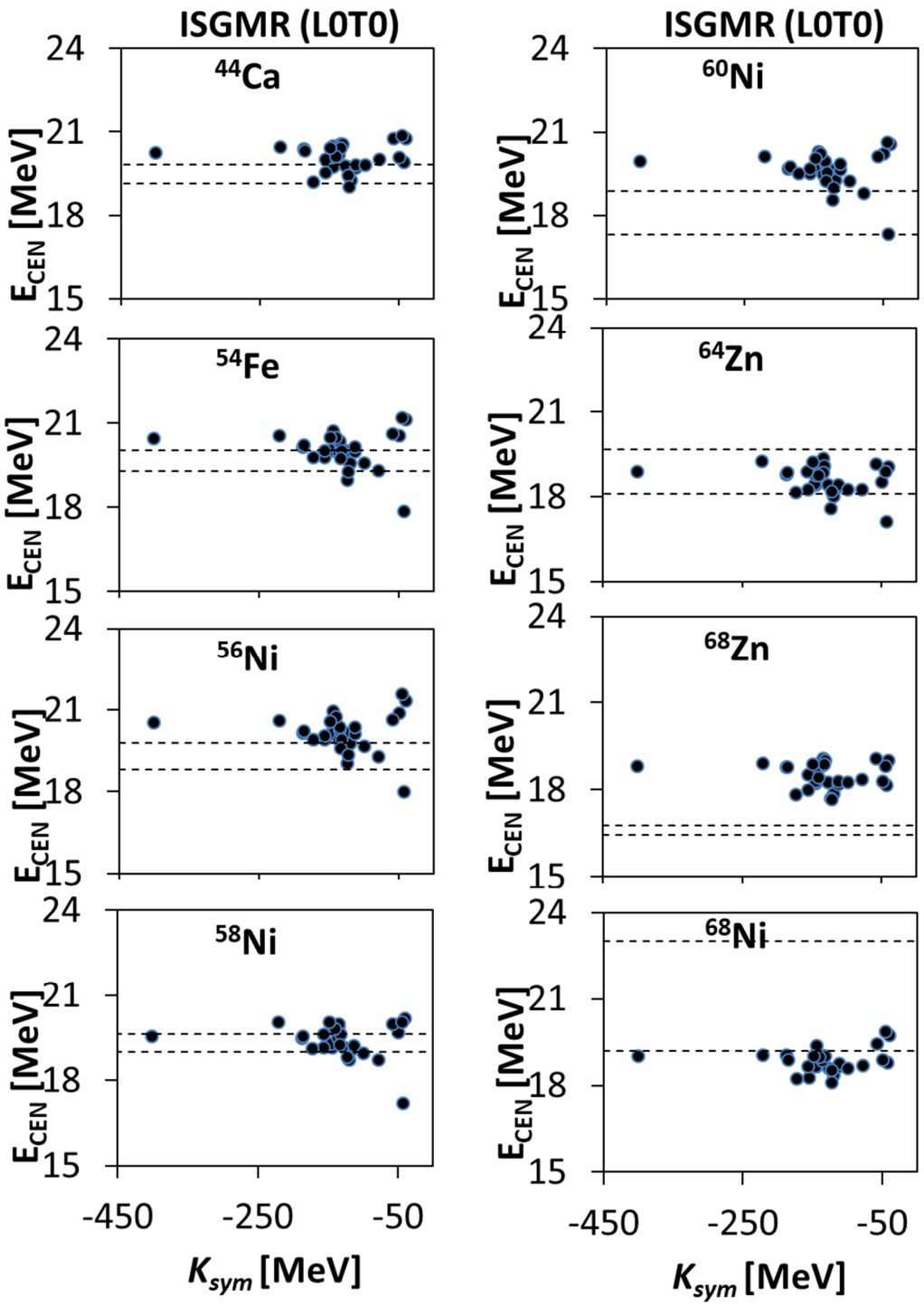

FIG. 4. As in FIG. 1 but we plot the centroid energy as a function of the 2nd derivative of the symmetry energy, K_{sym}, at saturation energy. No correlations are obtained for the theoretical values of E_{CEN} and K_{sym}, with C ~ 0.24.

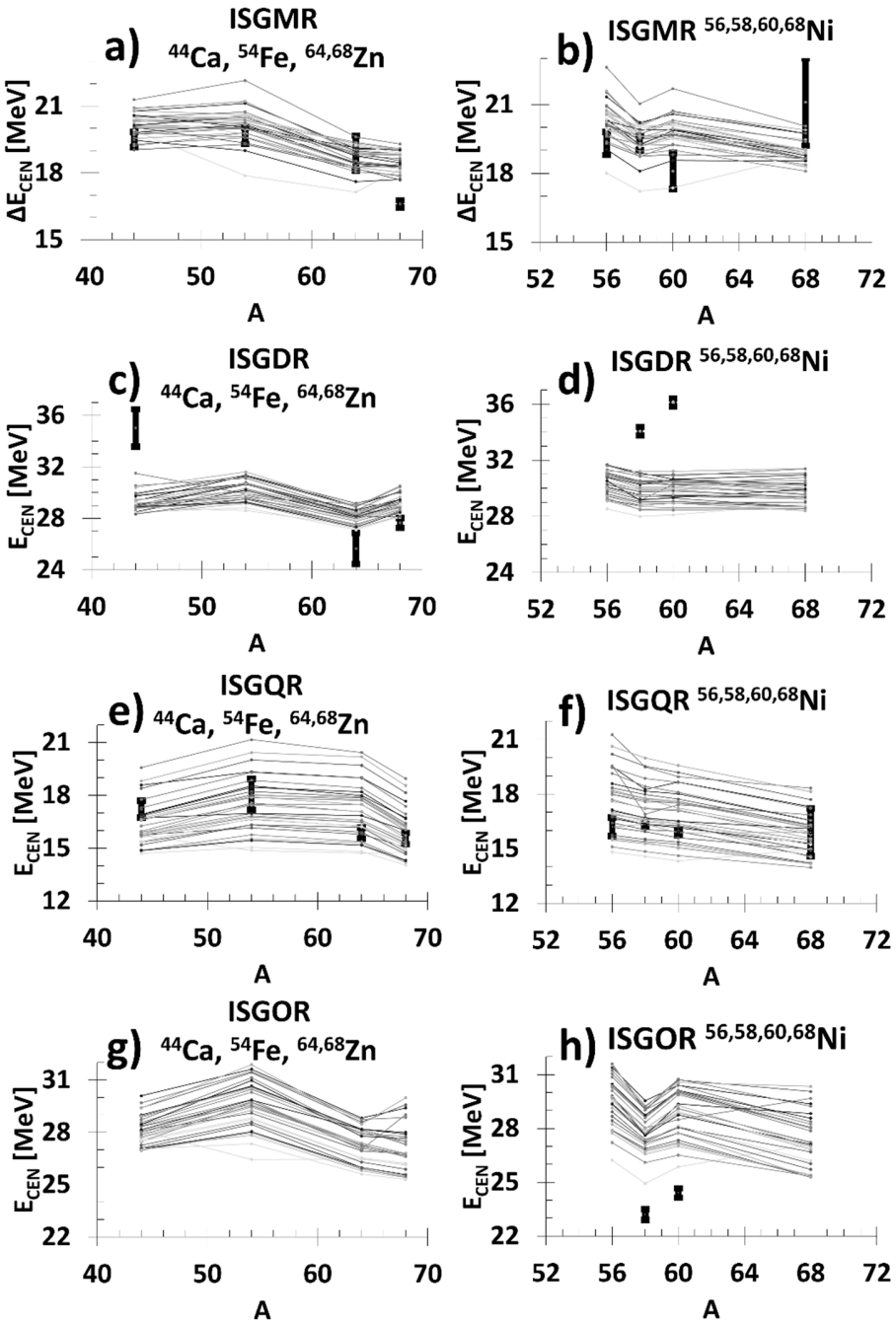

FIG. 5. The centroid energies [MeV] of the isoscalar giant resonances with multipolarities from L=0 to L=3 for ^{44}Ca, ^{54}Fe, and ^{64,68}Zn (left figures) and for ^{56,58,60,68}Ni (right figures), are plotted against the mass A of each isotope. The experimental error bars (where available) are shown by the solid vertical lines, while the theoretical values of E_{CEN} are shown as dots connected by lines (to guide the eye).

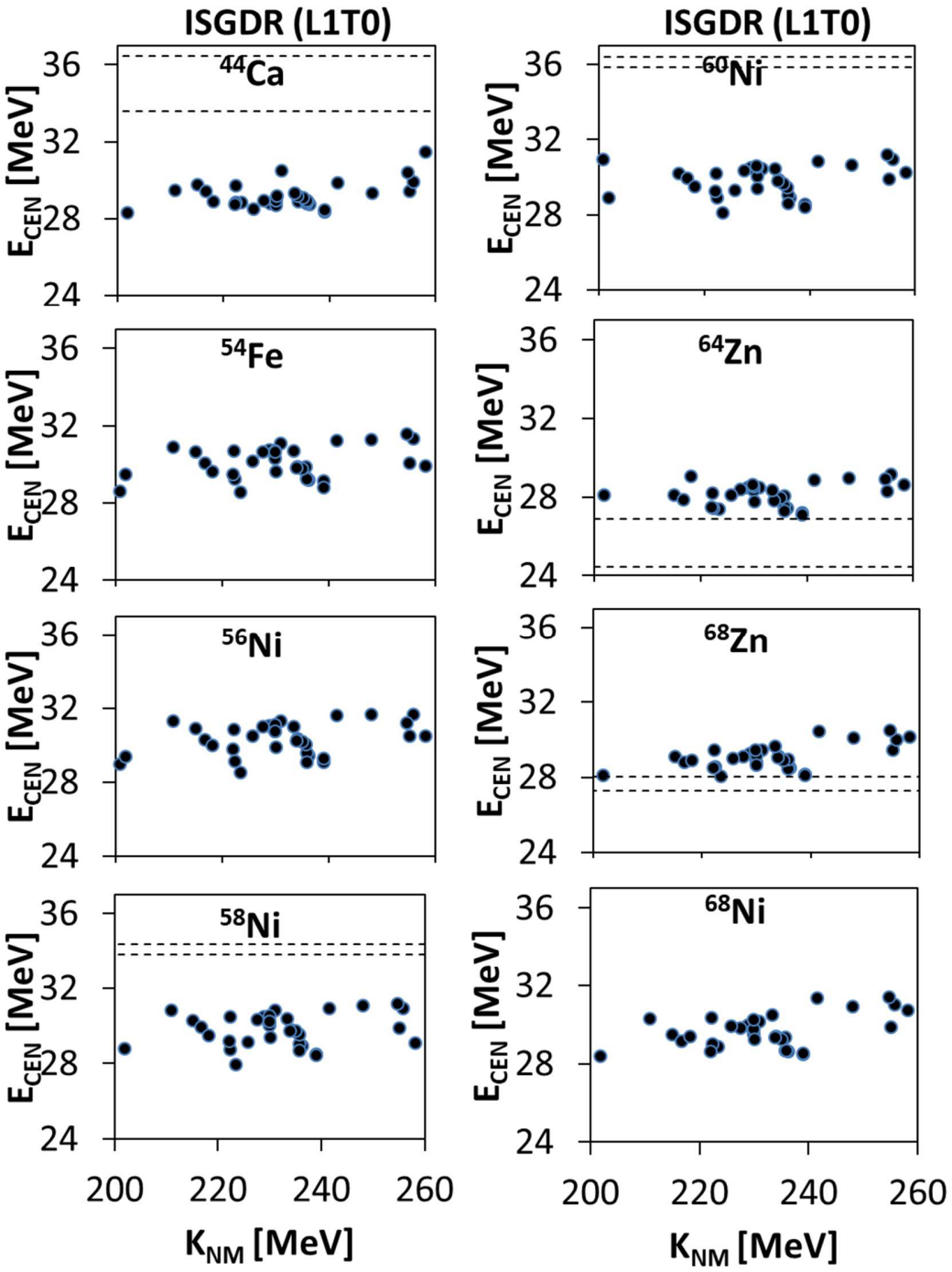

FIG. 6. As in FIG. 1 but we show the centroid energy as a function of the isoscalar giant dipole resonance plotted against the incompressibility coefficient $K_{NM,}$ for different nuclei. We find weak correlation between the calculated values of E_{CEN} and K_{NM} with a Pearson linear correlation coefficient C ~ 0.39, mostly due to the already recognized correlation between K_{NM} and m*/m shown in Table V of Ref.[11].

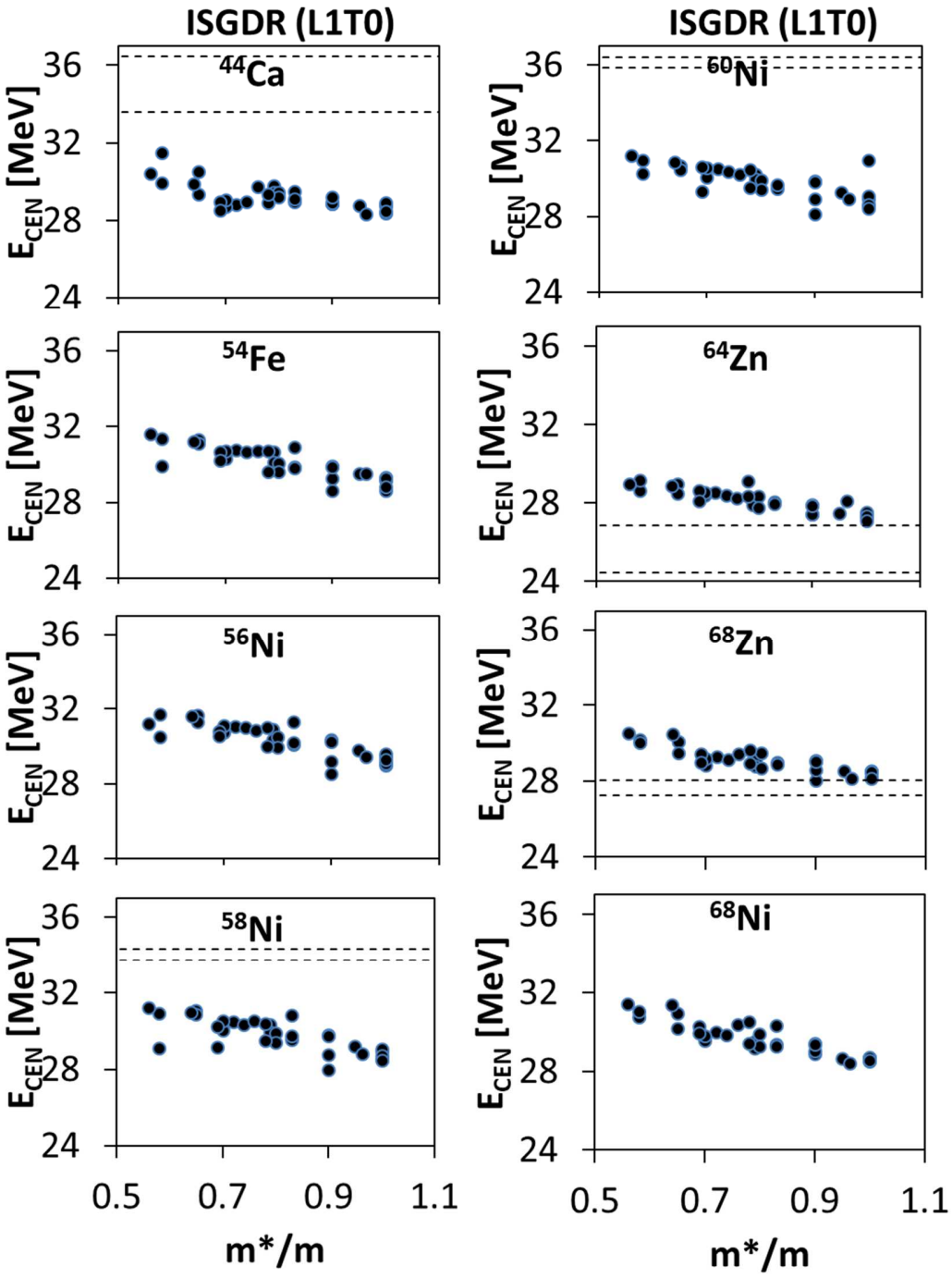

FIG. 7. As in FIG. 1 but we show the centroid energy of the ISGDR plotted against the effective mass for different nuclei. A strong correlation is obtained for the theoretical results of E_{CEN} and m^*/m, with C ~ -0.83 in all cases.

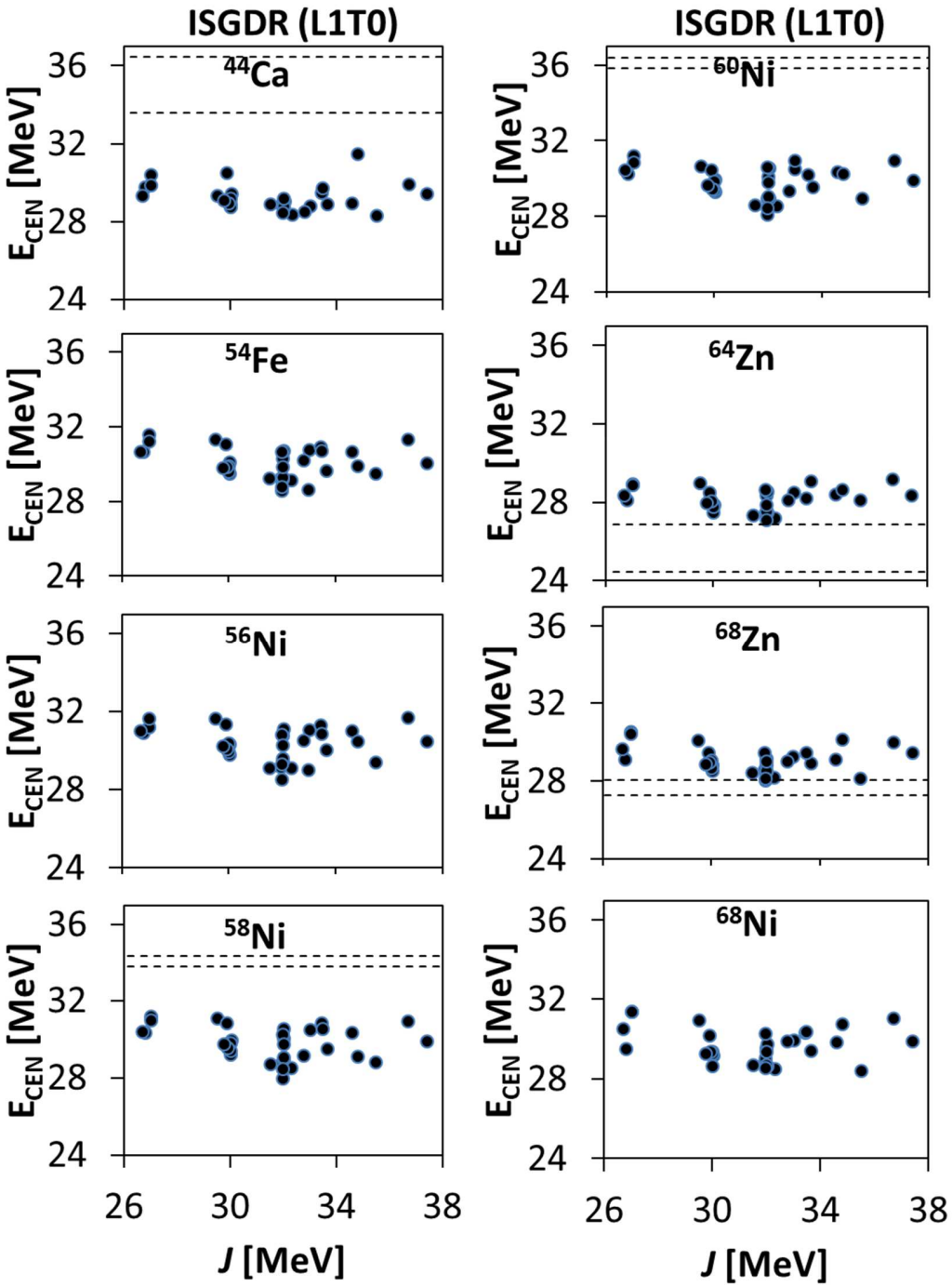

FIG. 8. As in FIG. 1 but we show the centroid energy of the ISGDR plotted against the symmetry energy, J, at saturation density for different nuclei. No correlation is obtained for the theoretical results of E_{CEN} and J (C ~ -0.17).

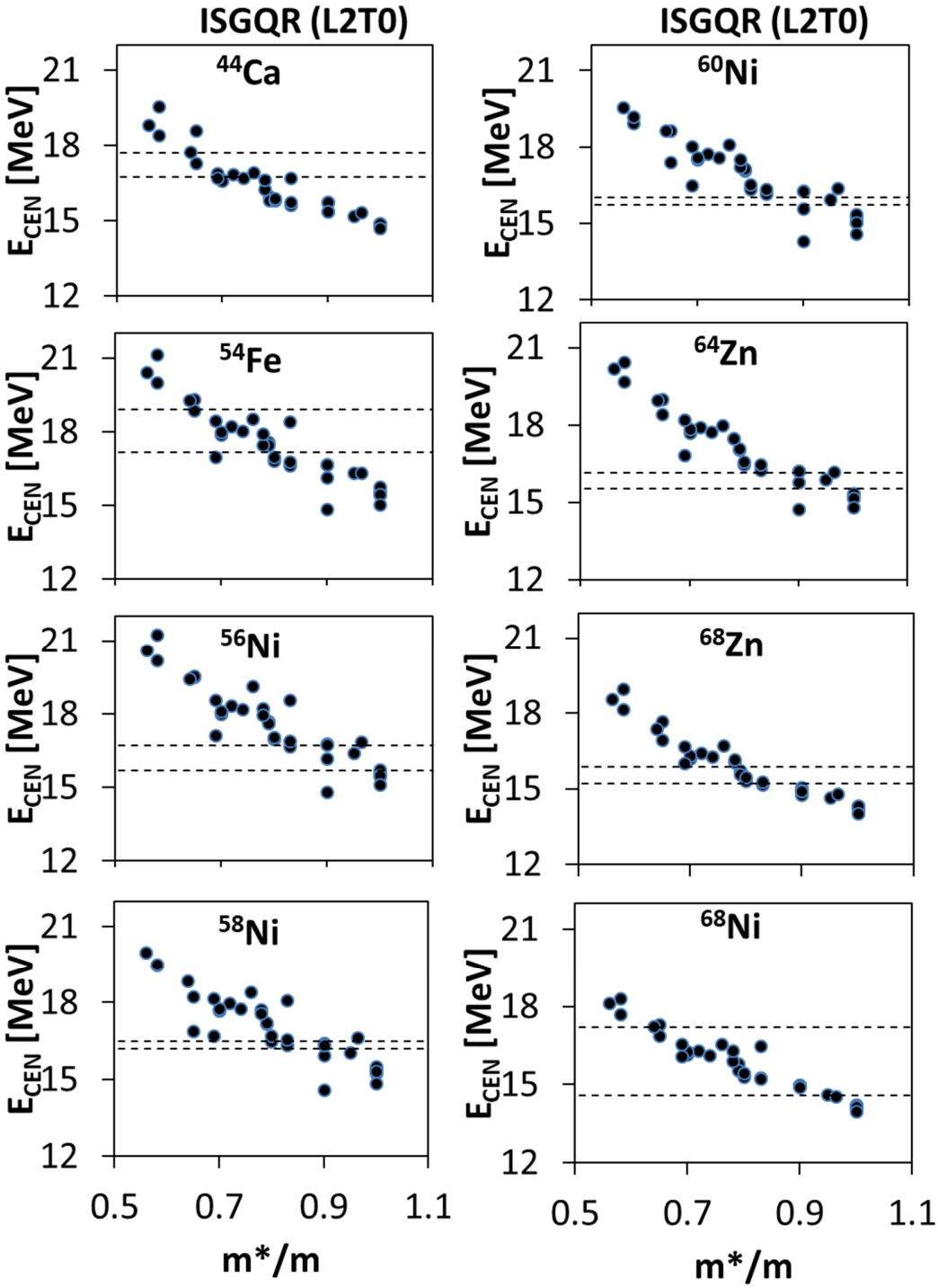

FIG. 9. As in FIG. 1 but we show the centroid energy of the ISGQR plotted against the effective mass. A strong correlation is found for the theoretical results of E_{CEN} and m*/m with C ~ -0.93.

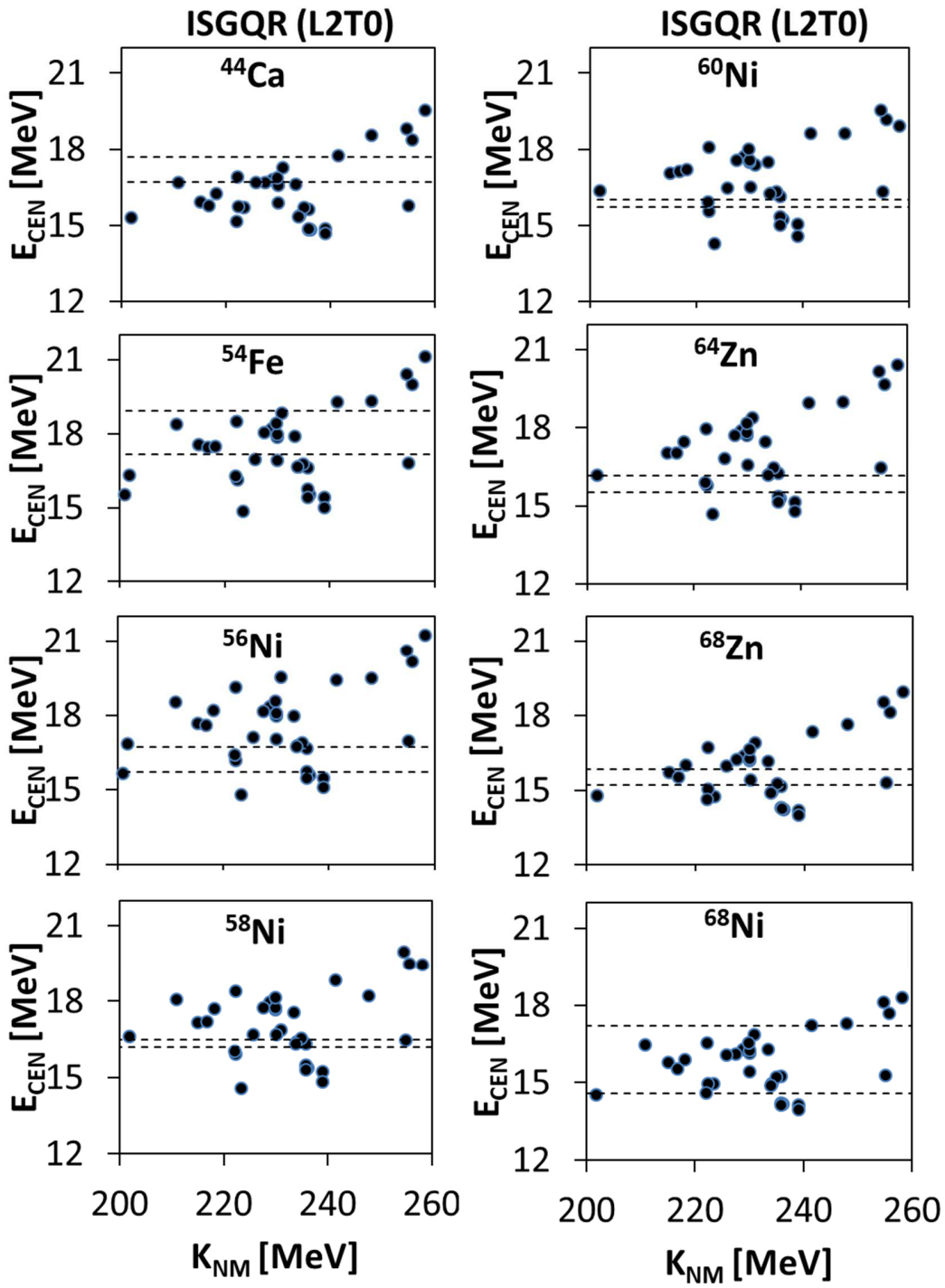

FIG. 10. As in FIG. 1 but we show the centroid energy of the ISGQR plotted against the incompressibility coefficient K_{NM}. We find weak correlation between the calculated values of K_{NM} and E_{CEN} with a Pearson linear correlation coefficient close to C ~ 0.40 for all isotopes, mostly due to the correlation between K_{NM} and m*/m shown in Table V of Ref.[11].

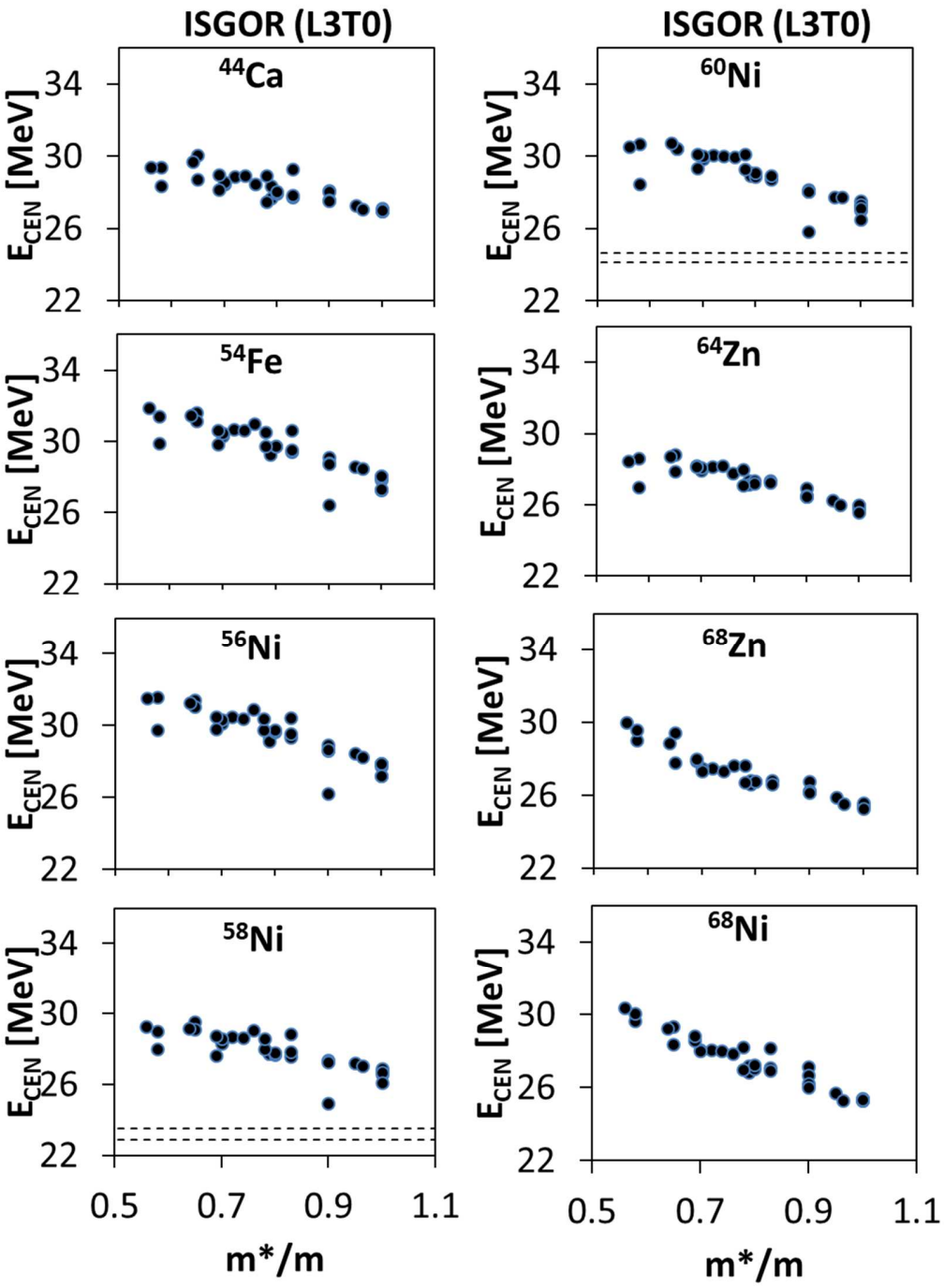

FIG. 11. As in FIG. 1 but we show the centroid energy of the ISGOR plotted against the effective mass. Strong correlations are found for the theoretical results of E_{CEN} and m*/m with C greater in magnitude than -0.89 for all nuclei considered.

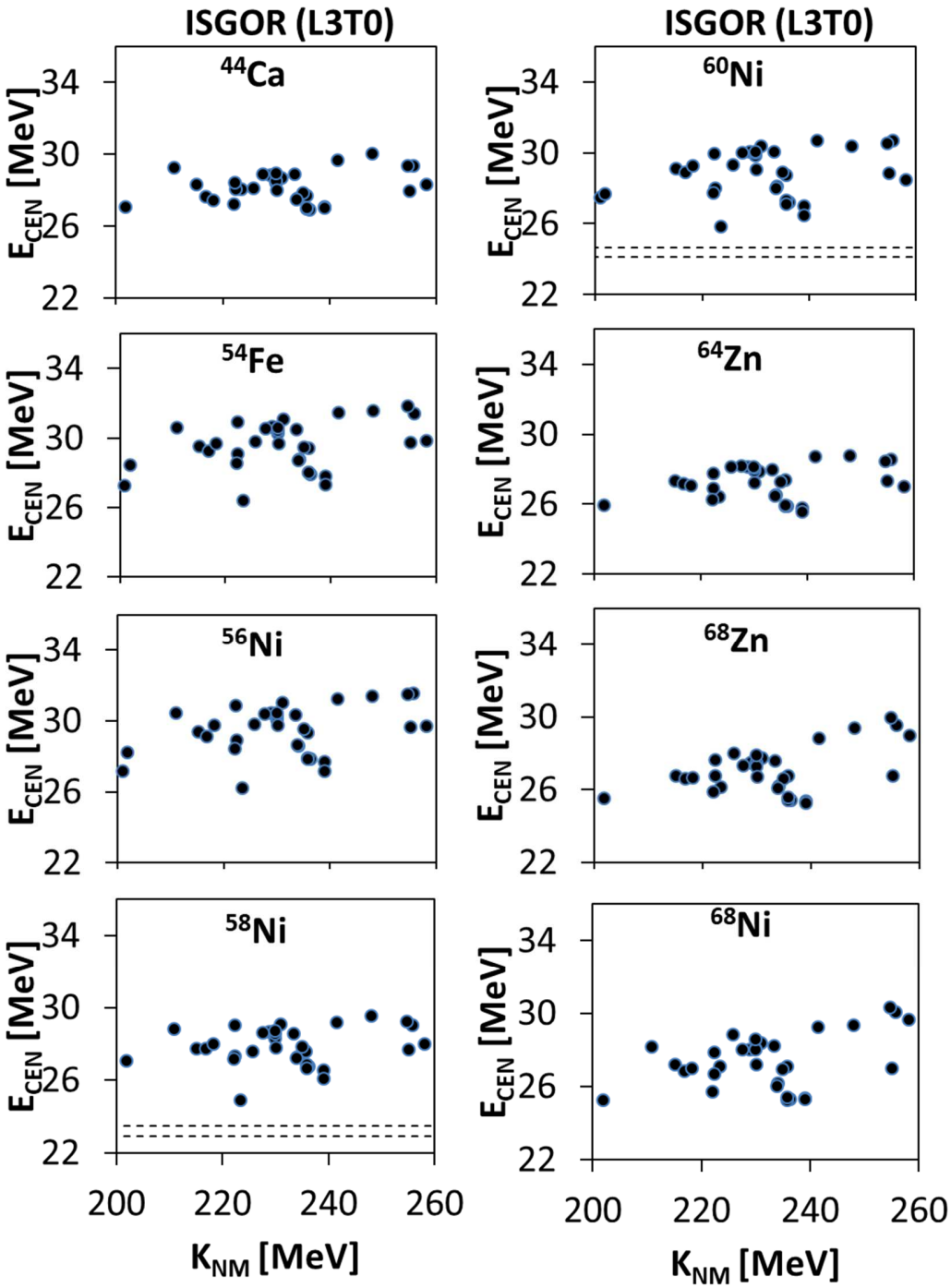

FIG. 12. As in FIG. 1 but we show the centroid energy of the ISGOR plotted against the incompressibility coefficient K_{NM}. We find no correlations for the centroid energies resulting from the HF-RPA calculations and the values of K_{NM} with C ~ 0.32.

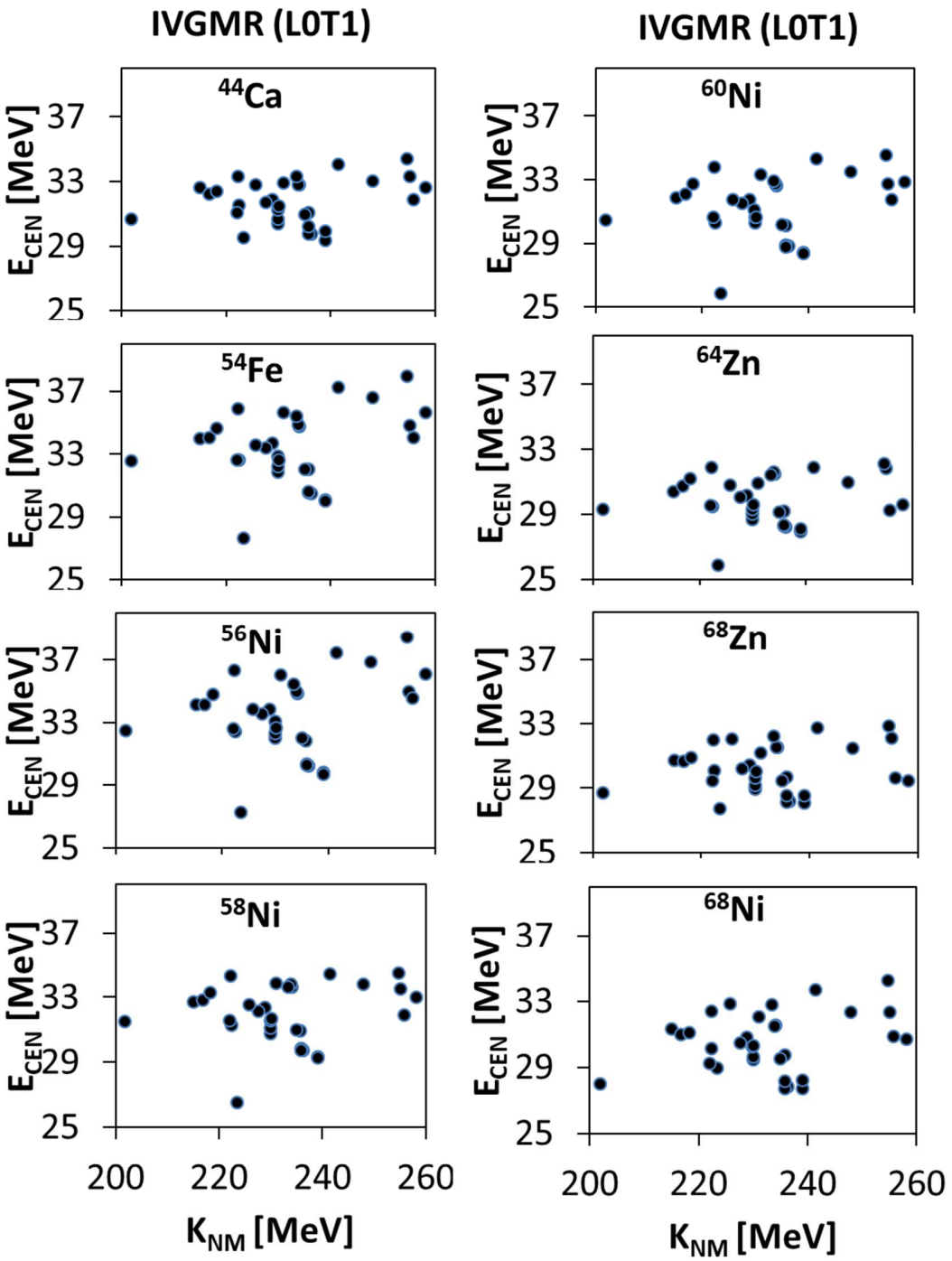

FIG. 13. As in FIG. 1 but we show the centroid energy of the IVGMR plotted against the incompressibility coefficient of nuclear matter, K_{NM}. No correlations are found for the theoretical centroid energies, resulting from the HF-RPA, and K_{NM} with C ~ 0.22.

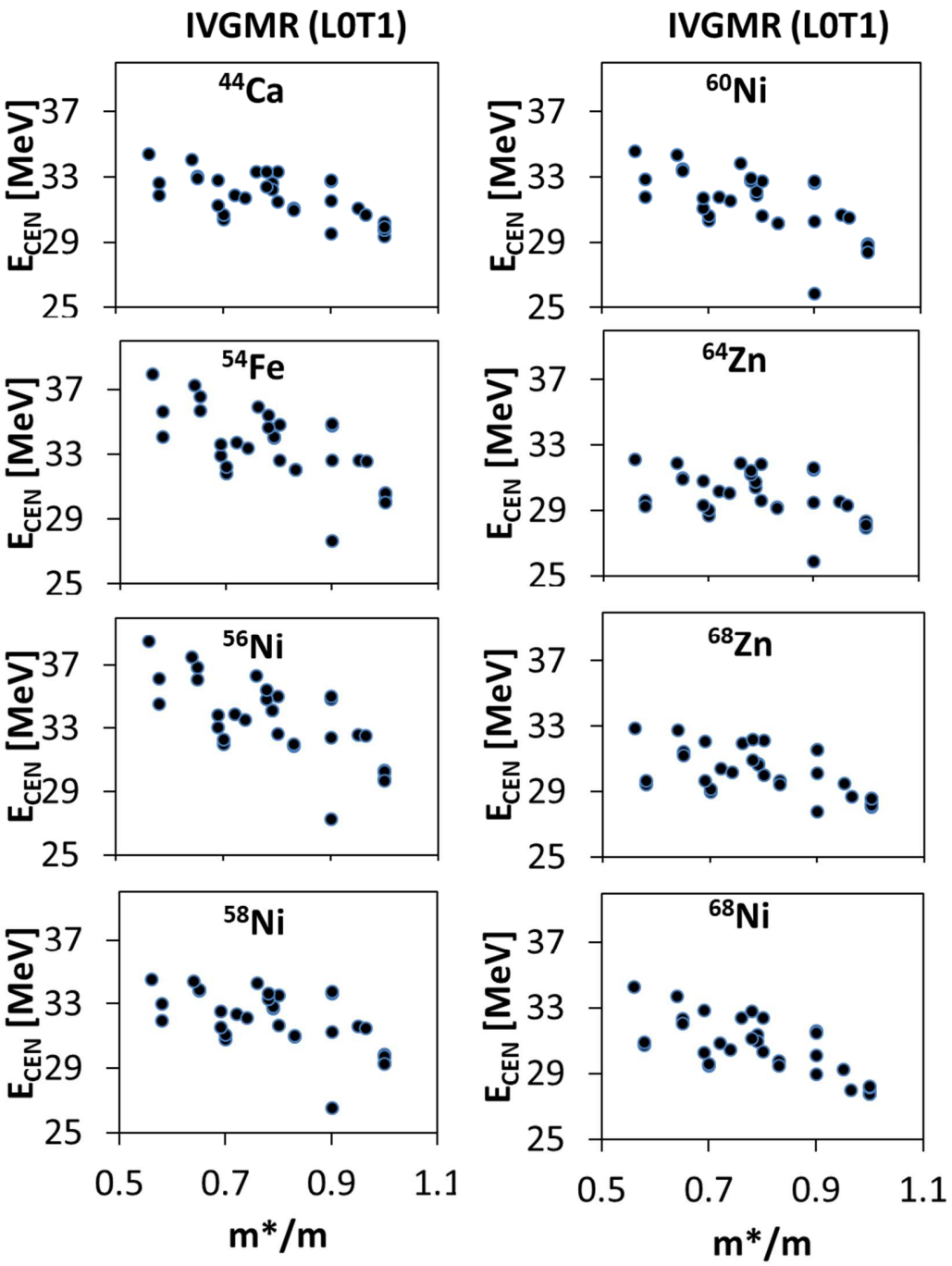

FIG. 14. As in FIG. 1 but we show the centroid energy of the IVGMR plotted against the effective mass. We found medium correlations between the calculated values of E_{CEN} and m*/m with C ~ -0.64 for all the isotopes studied here.

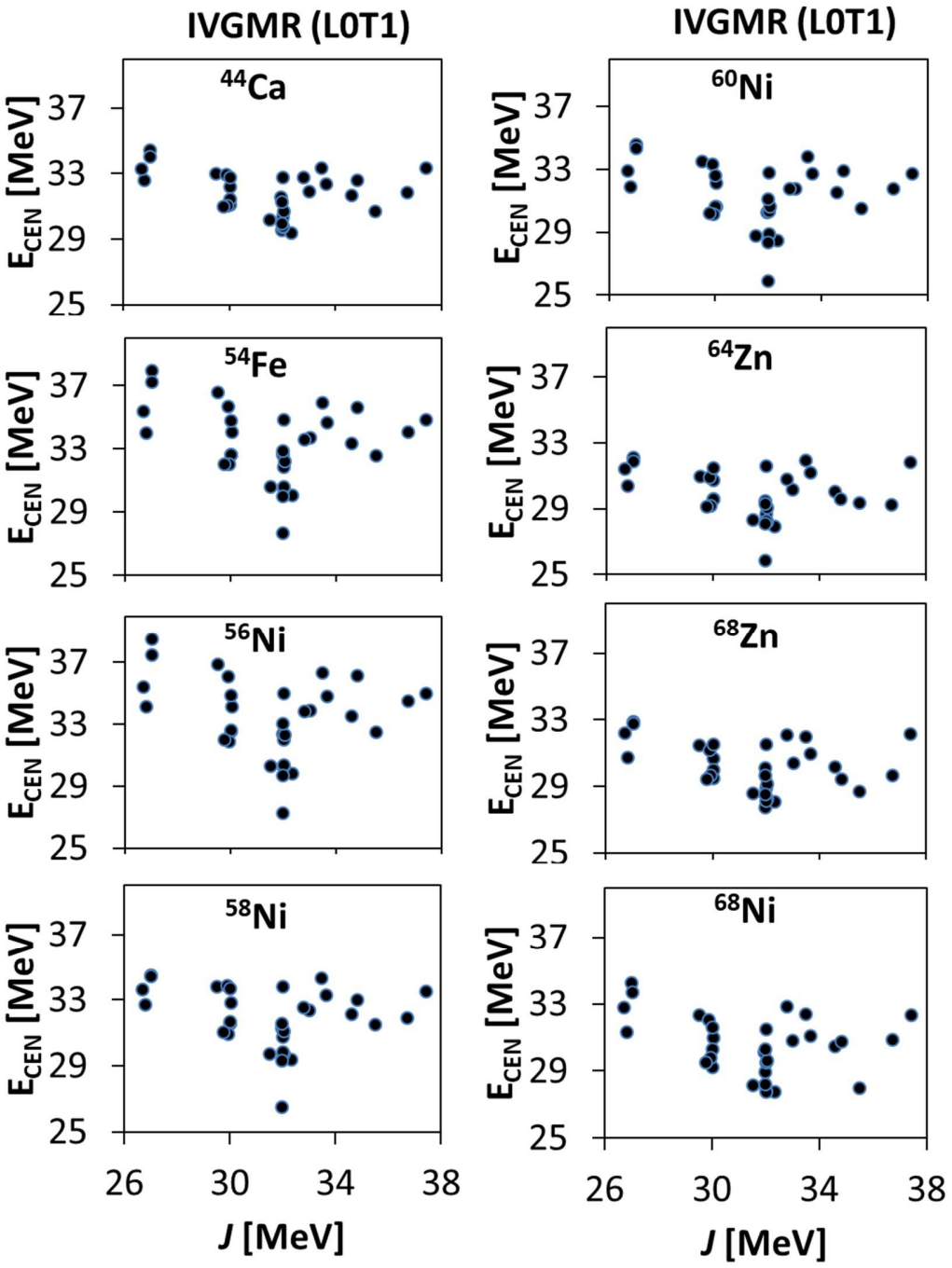

FIG. 15. As in FIG. 1 but we show the centroid energy of the IVGMR plotted against the symmetry coefficient, J, at saturation density. No correlations are obtained for the centroid energies resulting from the HF-RPA calculations and J, with C ~ -0.24.

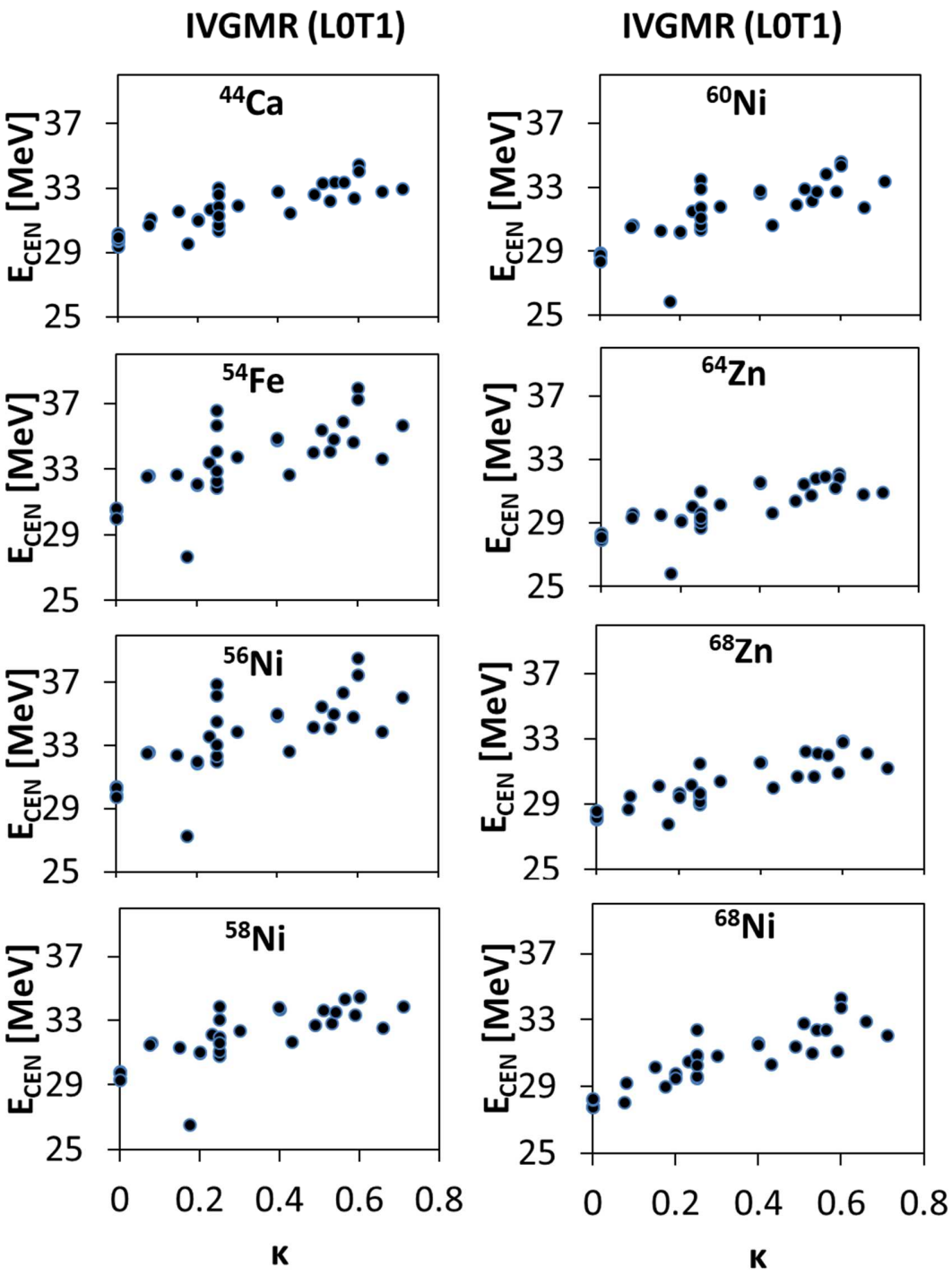

FIG. 16. As in FIG. 1 but we show the theoretical centroid energies of the IVGMR plotted against the enhancement coefficient, κ, of the energy weighted sum rule (EWSR) of the isovector giant dipole resonance (IVGDR). We find strong correlation between the calculated value of κ and E_{CEN} with a Pearson linear correlation coefficient C ~ 0.80 for all isotopes considered.

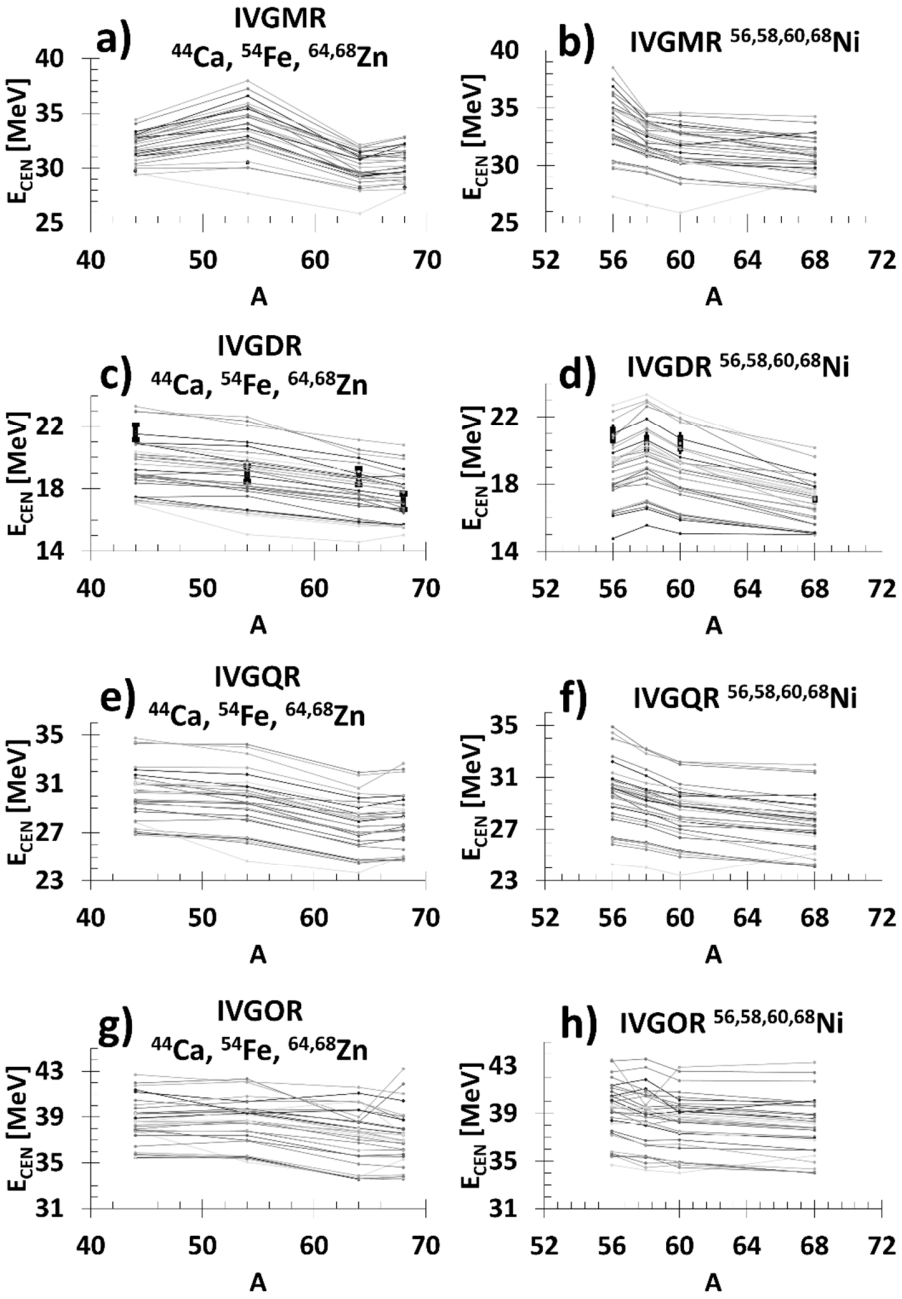

FIG. 17. The centroid energies [MeV] of the isovector giant resonances of multipolarities from L=0 to L=3 for ^{44}Ca, ^{54}Fe, and ^{64,68}Zn (left figures) and for ^{56,58,60,68}Ni (right figures), are plotted against the mass A of each isotope. The experimental error bar (where available) are shown by the solid vertical lines, while the theoretical values of E_{CEN} are shown as dots connected by lines (to guide the eye).

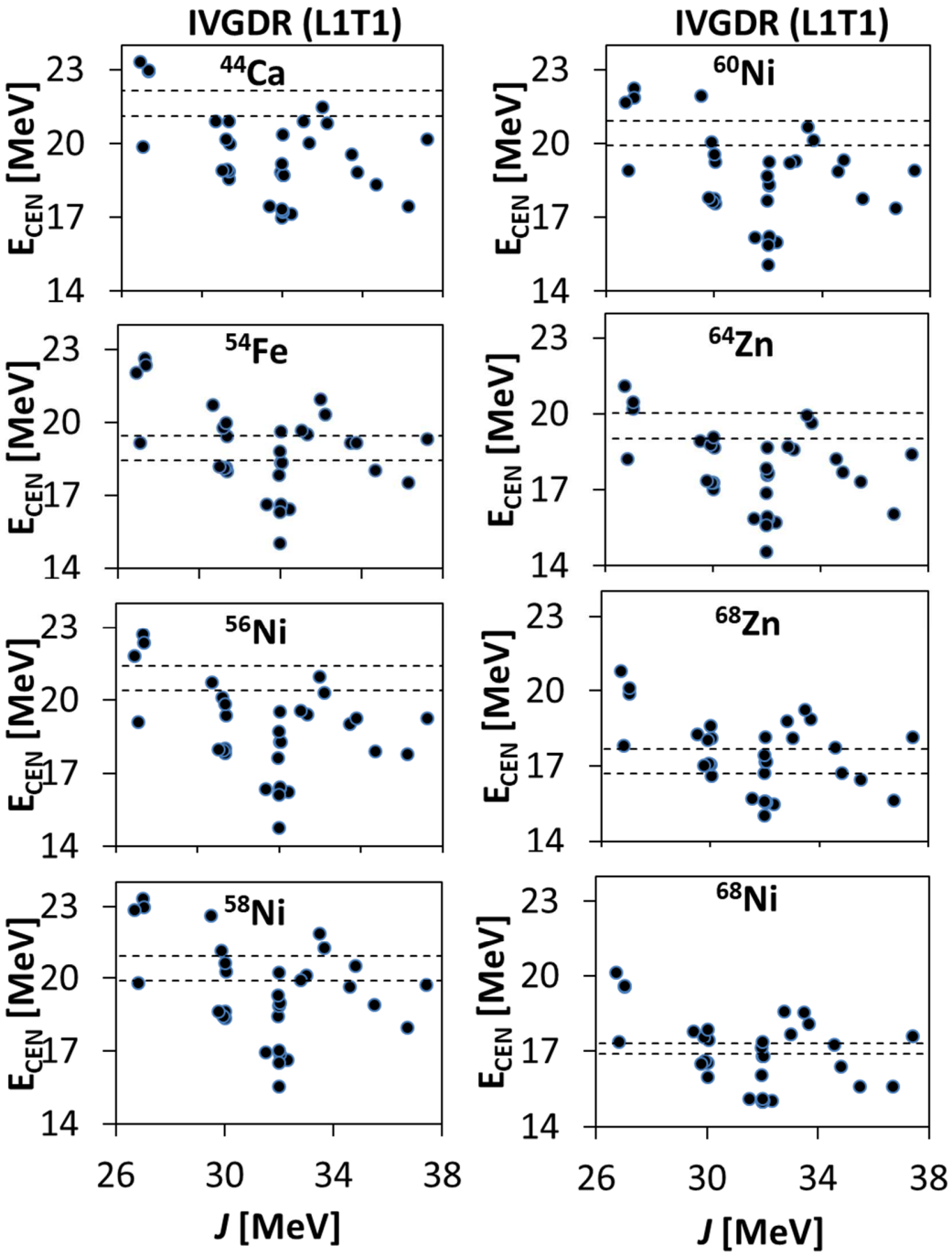

FIG. 18. As in FIG. 1 but we show the theoretical centroid energies of the IVGDR plotted against the symmetry energy, J. Weak correlations were found between the values of the centroid energies resulting from the HF-RPA calculations and J, with C ~ -0.39.

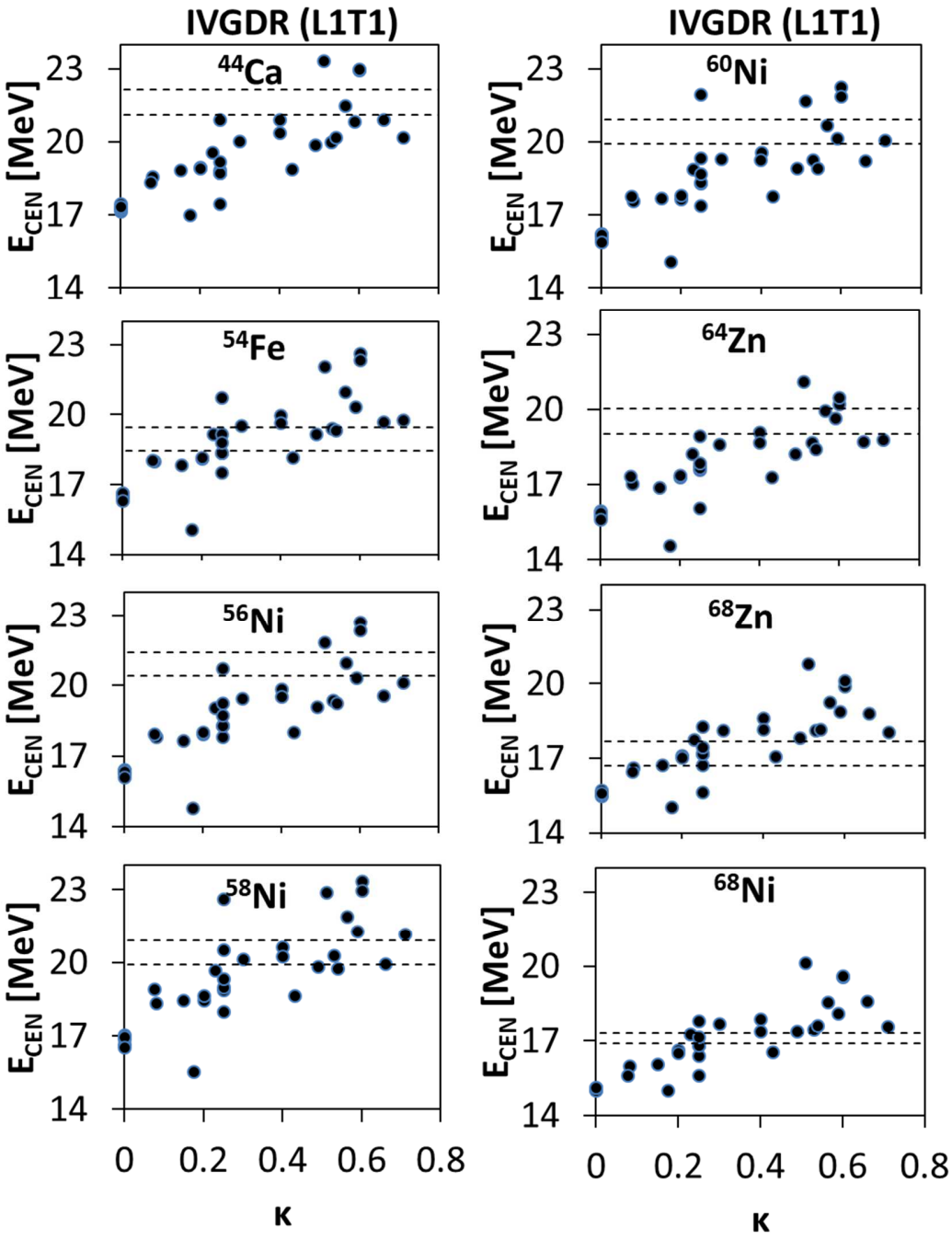

FIG. 19. As in FIG. 1 but we show the theoretical centroid energies of the IVGDR plotted against the energy weighted sum rule enhancement coefficient κ of the IVGDR. We find strong correlation between the calculated values of κ and E_{CEN} with a Pearson linear correlation coefficient C ~ 0.80 for all isotopes considered.

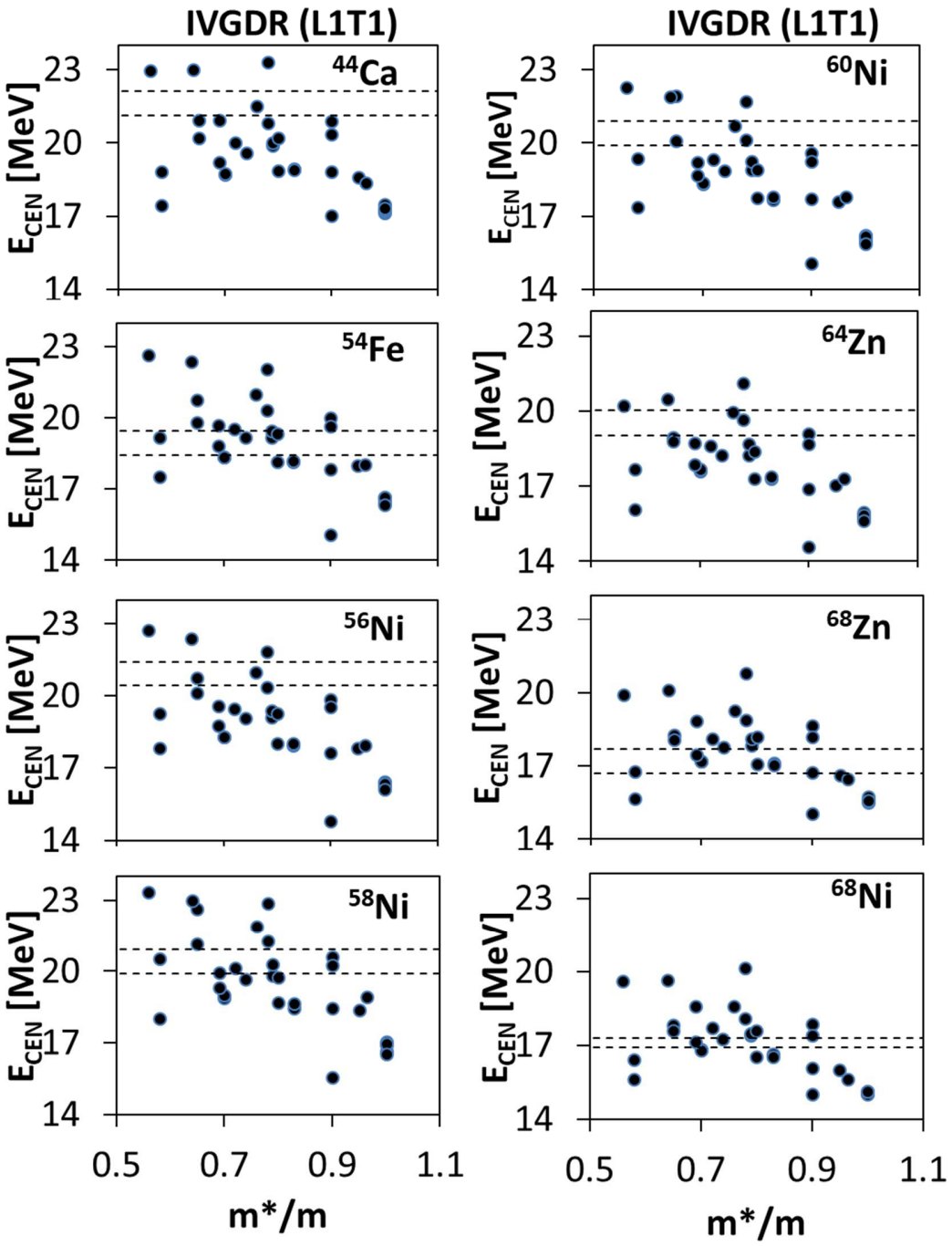

FIG. 20. As in FIG. 1 but we show the theoretical centroid energies of the IVGDR plotted against the effective mass m*/m. Medium correlations were found between the centroid energies, resulting from the theoretical HF-RPA calculations, and m*/m with C ~ -0.62 for the isotopes investigated here.

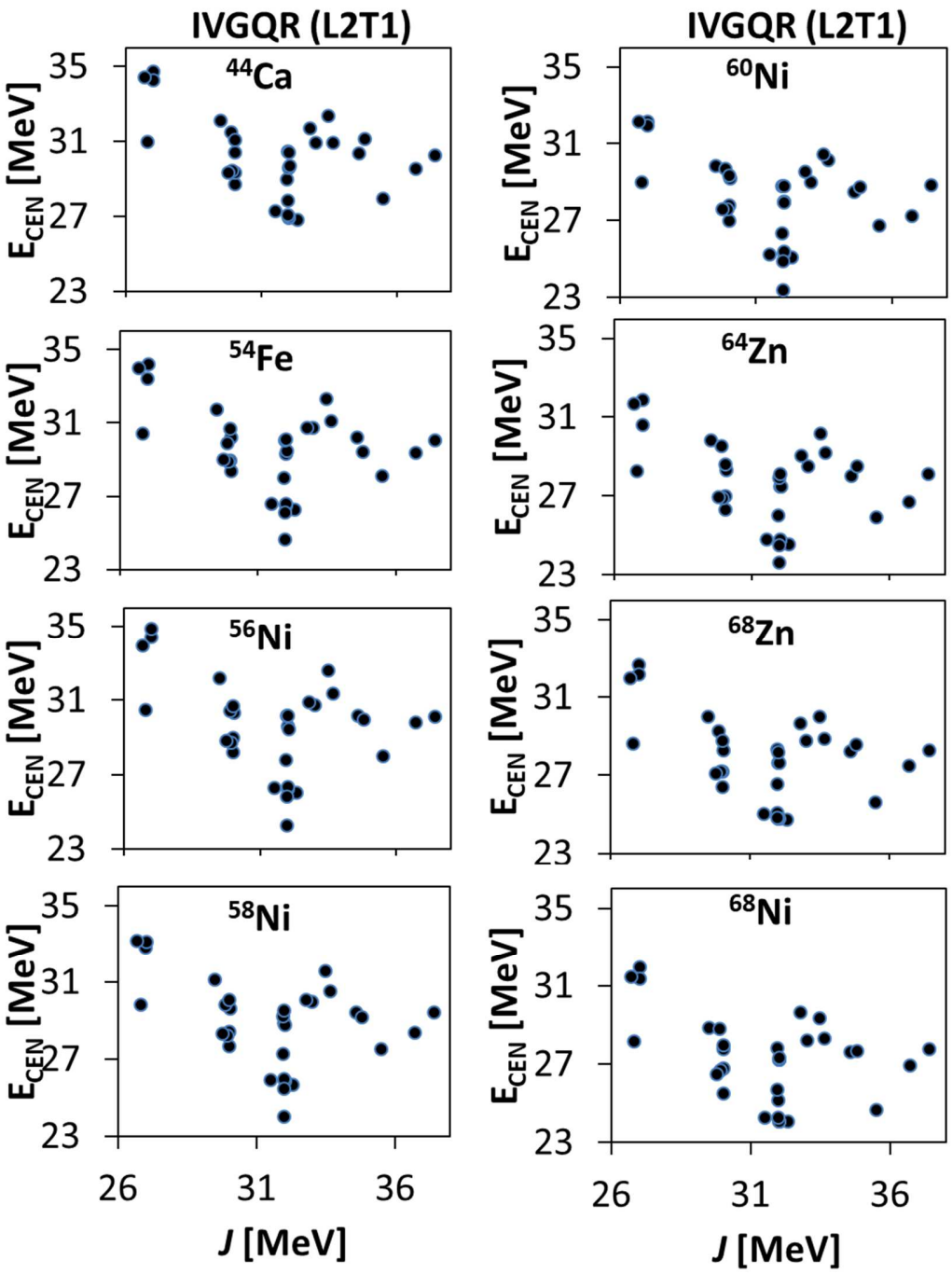

FIG. 21. As in FIG. 1 but we show the theoretical centroid energies of the IVGQR plotted against the symmetry energy, J. Weak correlations were obtained for the centroid energies, resulting from the theoretical HF-RPA calculations, and the value of J, with C ~ -0.38.

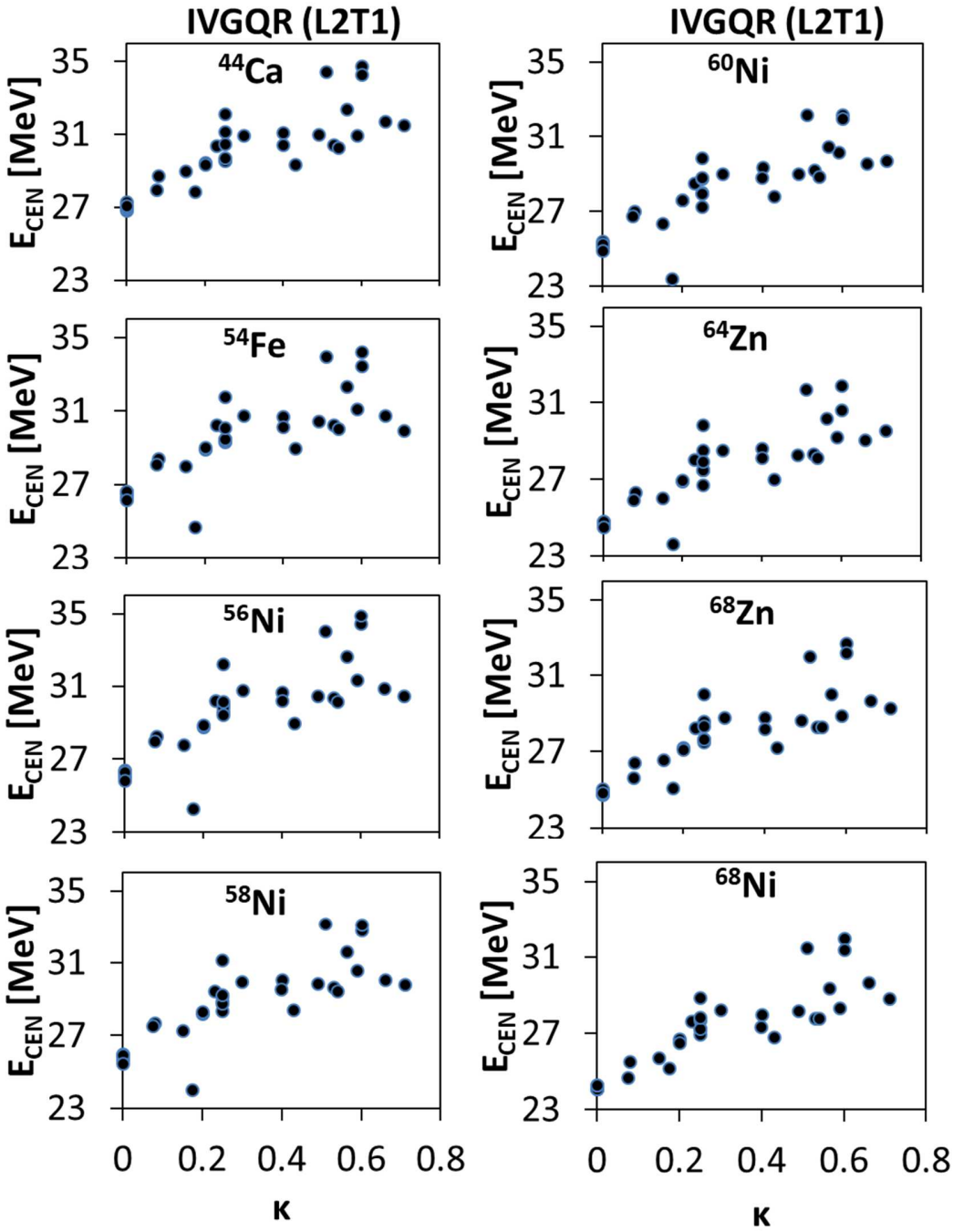

FIG. 22. As in FIG. 1 but we show the theoretical centroid energies of the IVGQR plotted against the enhancement coefficient, κ, of the EWSR of the IVGDR. Strong correlations were obtained for the centroid energies, resulting from the theoretical HF-RPA calculations, and the values of κ, with C ~ 0.81 for the isotopes investigated here.

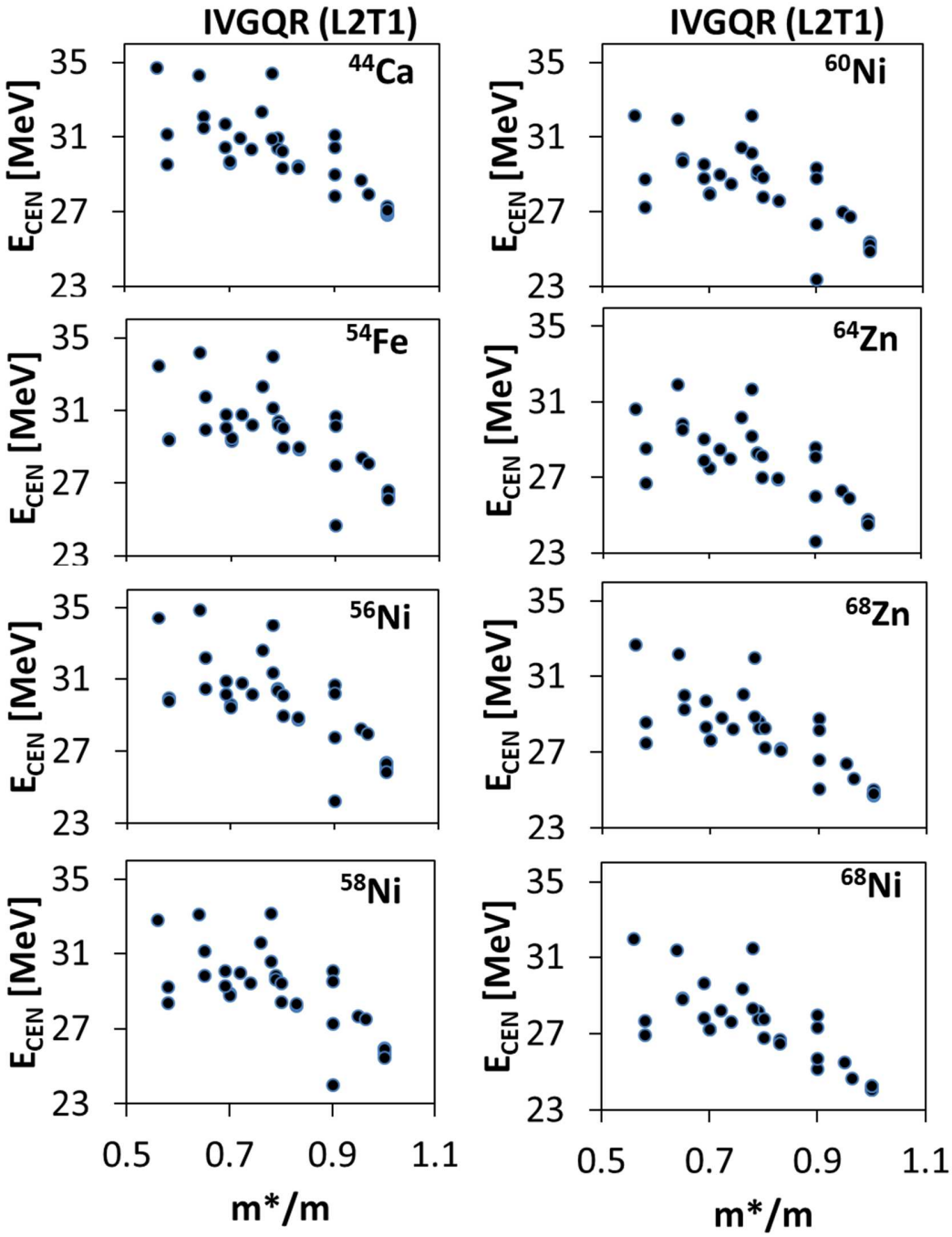

FIG. 23. As in FIG. 1 but we show the theoretical centroid energies of the IVGQR for different nuclei plotted against the effective mass m*/m. Medium correlations were obtained for the centroid energies, resulting from the theoretical HF-RPA calculations, and m*/m, with C ~ -0.73 for the nuclei investigated in this work.

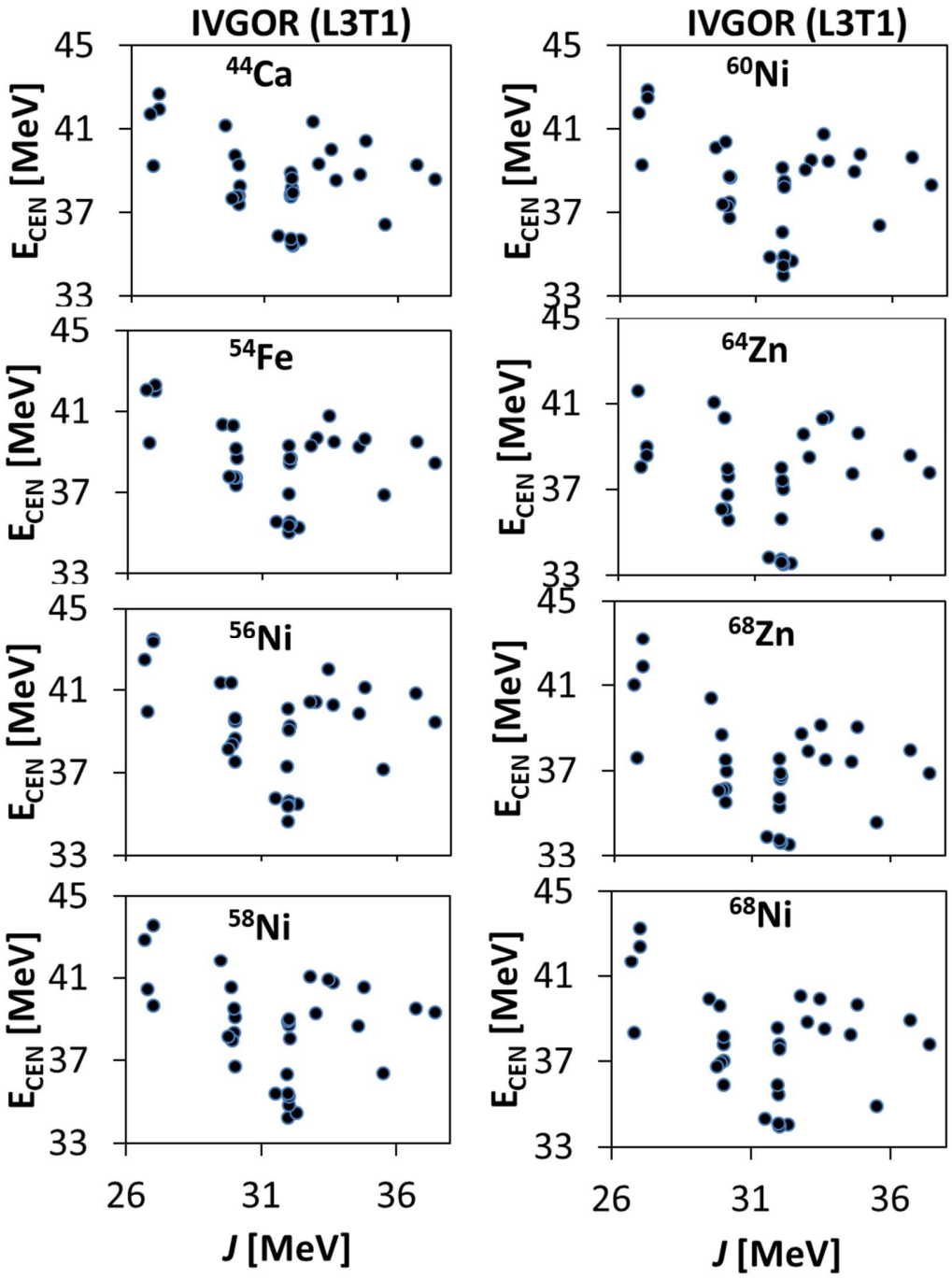

FIG. 24. As in FIG. 1 but we show the theoretical centroid energies of the IVGOR for different nuclei plotted against the symmetry energy J. No correlations are obtained for the centroid energies, resulting from the theoretical HF-RPA calculations, and J with C ~ -0.29.

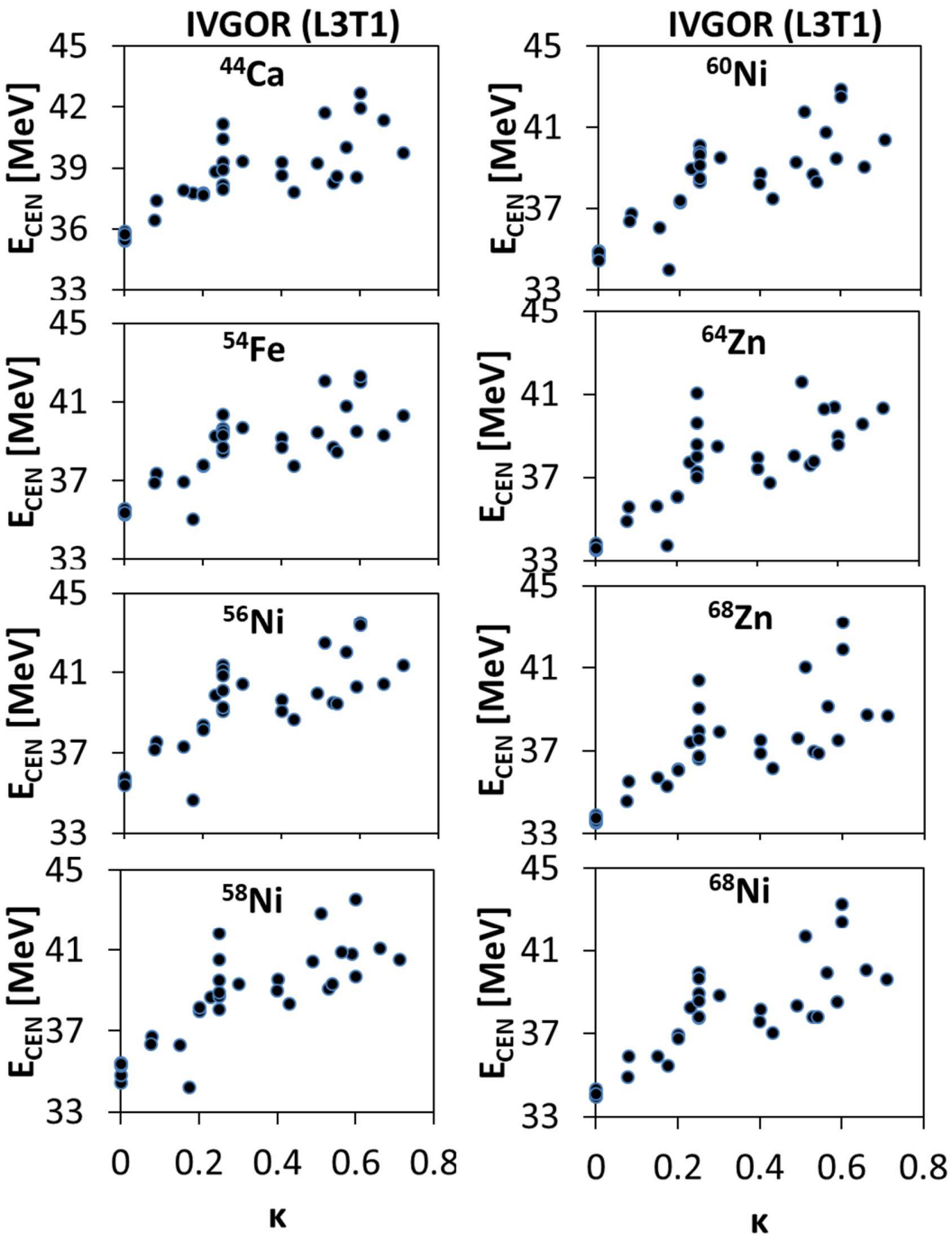

FIG. 25. As in FIG. 1 but we show the theoretical centroid energies of the IVGOR for different nuclei plotted against κ. Medium correlations are obtained for the centroid energies, resulting from the theoretical HF-RPA calculations, and the values of κ with C ~ 0.79 for the nuclei investigated in this work.

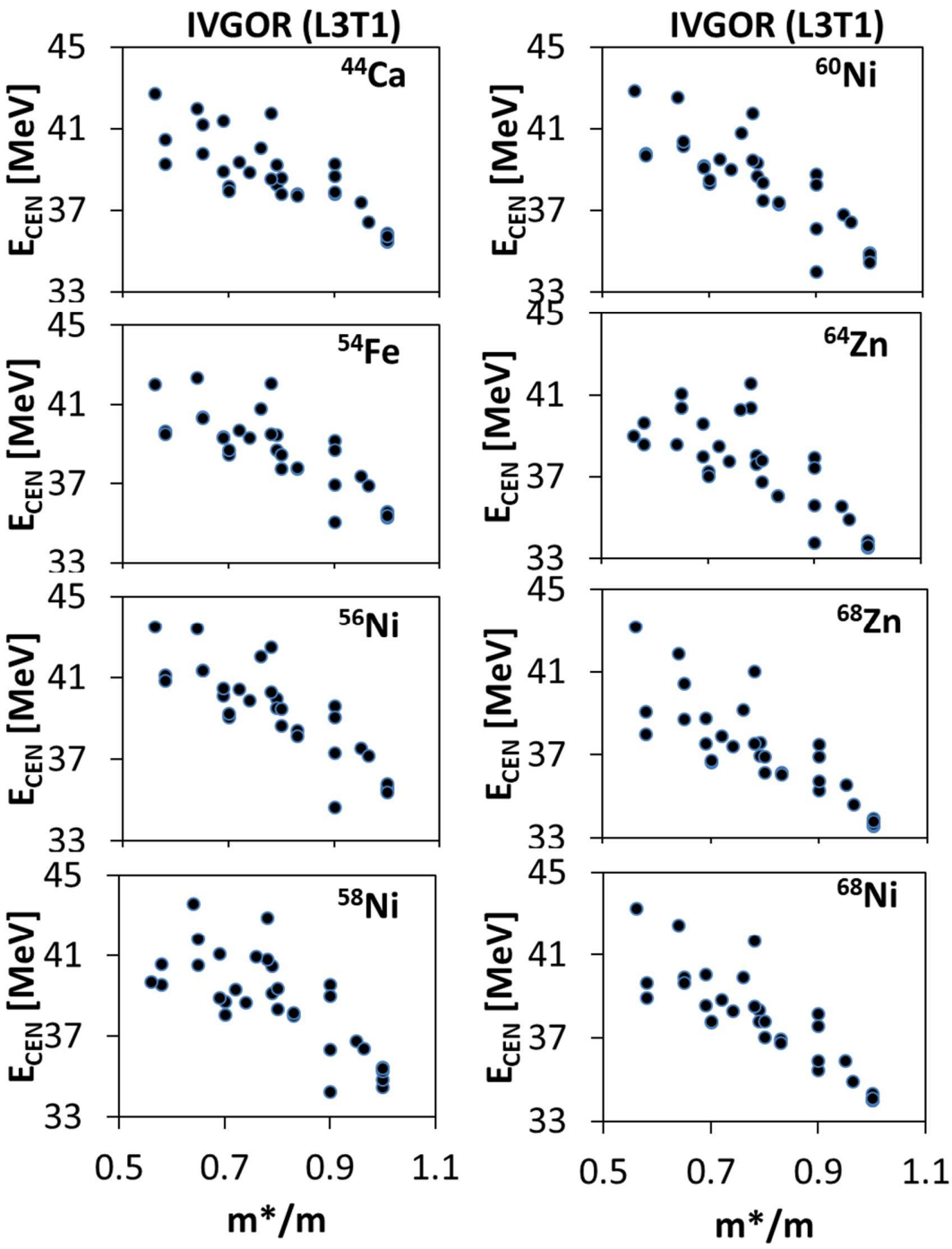

FIG. 26. As in FIG. 1 but we show the theoretical centroid energies of the IVGOR for different nuclei plotted against the effective mass. Strong correlations are obtained for the centroid energies, resulting from the theoretical HF-RPA calculations, and the values of m*/m with C ~ -0.82 for the nuclei investigated in this work.